macromol

MDPI

Review

Chitosan Adsorbent Derivatives for Pharmaceuticals Removal from Effluents: A Review

Efstathios V. Liakos [1], Maria Lazaridou [2], Georgia Michailidou [2], Ioanna Koumentakou [2], Dimitra A. Lambropoulou [3], Dimitrios N. Bikiaris [2] and George Z. Kyzas [1,*]

[1] Department of Chemistry, International Hellenic University, 65404 Kavala, Greece; stathilas@gmail.com
[2] Laboratory of Polymer Chemistry and Technology, Department of Chemistry, Aristotle University of Thessaloniki, GR-541 24 Thessaloniki, Greece; marlazach@chem.auth.gr (M.L.); michailidougeorgia18@gmail.com (G.M.); iwanna.koumentakou@gmail.com (I.K.); dbic@chem.auth.gr (D.N.B.)
[3] Laboratory of Environmental Pollution Control, Department of Chemistry, Aristotle University of Thessaloniki, GR-541 24 Thessaloniki, Greece; dlambro@chem.auth.gr
* Correspondence: kyzas@chem.ihu.gr; Tel.: +30-2510-462-218

Abstract: Chitin is mentioned as the second most abundant and important natural biopolymer in worldwide scale. The main sources for the extraction and exploitation of this natural polysaccharide polymer are crabs and shrimps. Chitosan (poly-β-(1 → 4)-2-amino-2-deoxy-d-glucose) is the most important derivative of chitin and can be used in a wide variety of applications including cosmetics, pharmaceutical and biomedical applications, food, etc., giving this substance high value-added applications. Moreover, chitosan has applications in adsorption because it contains amino and hydroxyl groups in its molecules, and can thus contribute to many possible adsorption interactions between chitosan and pollutants (pharmaceuticals/drugs, metals, phenols, pesticides, etc.). However, it must be noted that one of the most important techniques of decontamination is considered to be adsorption because it is simple, low-cost, and fast. This review emphasizes on recently published research papers (2013–2021) and briefly describes the chemical modifications of chitosan (grafting, cross-linking, etc.), for the adsorption of a variety of emerging contaminants from aqueous solutions, and characterization results. Finally, tables are depicted from selected chitosan synthetic routes and the pH effects are discussed, along with the best-fitting isotherm and kinetic models.

Keywords: chitosan; synthesis; characterization; pH; isotherms; adsorption capacity; kinetics

Citation: Liakos, E.V.; Lazaridou, M.; Michailidou, G.; Koumentakou, I.; Lambropoulou, D.A.; Bikiaris, D.N.; Kyzas, G.Z. Chitosan Adsorbent Derivatives for Pharmaceuticals Removal from Effluents: A Review. *Macromol* **2021**, *1*, 130–154. https://doi.org/10.3390/macromol1020011

Academic Editor: Luc Avérous

Received: 12 April 2021
Accepted: 1 May 2021
Published: 11 May 2021

1. Introduction

Emerging contaminants (ECs) may be defined as compounds that are not currently covered by existing water regulations but are thought to be a threat to environmental ecosystems and human beings. The presence of pharmaceuticals, even in low concentrations, constitute a danger to human and animal and to aquatic species. The widespread incidence of pharmaceuticals in water brings into light the inadequacy of conventional methods of water treatment and the necessity of developing alternative technologies for the optimization of the removal process. Particularly, the pharmaceutical compounds have been found in all aquatic environments (river, lakes, etc.), groundwater, and wastewater plant effluents in several countries, making it a significant environmental issue [1].

Chitosan (poly-β-(1→4)-2-amino-2-deoxy-D-glucose), the second most abundant biopolymer in nature after cellulose, is a polysaccharide produced by N-deacetylation of chitin [2]. Chitin exists in marine media and especially in the exoskeleton of crustaceans, or cartilages of mollusks, cuticles of insects and cell walls of microorganisms. Chitosan is a promising material not only for the remarkable properties such as biodegradability, biocompatibility, and antimicrobial activity but also for its adsorption capacity, as its cationic character enable it to interact with other molecules. The presence of amino and hydroxyl

groups on the structure makes possible the chemical modification of chitosan with the purpose of improving its solubility and electric change [3]. Furthermore, the modification of chitosan aims to ameliorate the surface area, hydrophilicity, and hydrolysability in acidic conditions, which remain some of the main disadvantages of this biopolymer. In the case of adsorption, which is considered the most promising separation technique [4–10], the modification of chitosan/or its composites is expected to fabricate materials, mainly with high surface area, mechanical strength, and functional groups for binding with the contaminants [11].

Our work provides a summary of the recently published studies (2013–2021) based on several forms of chitosan and modified derivatives as adsorbents for pharmaceutical compounds in aquatic environments. Taking into account the curiosity of the problem faced by modern societies and the lack of data, we emphasize the need to investigating new, eco-friendly adsorbents and study their capacity to separate pollutants from water.

2. Synthetic Routes and Characterizations

2.1. Chitosan/Modified Chitosan Beads

One acceptable form of chitosan (CS) used for the removal of pharmaceutical compounds is CS beads using the method of insoluble gelation. Studies showed that CS gelation beads (via adding chitosan solution to an alkaline non-solvent) is an efficient way to separate adsorbents with high affinity to contaminants. However, in order to enhance the acid resistance and mechanical properties, cross-linkers such as glutaraldehyde (GA), epichlorohydrin (EP), and glycol diglycidyl ether were used, which also influences the adsorption capacity. Lu et al. propose the utilization of chitosan beads grafted by polyethylenimine (PEI) and further cross-linked with glutaraldehyde and epichlorohydrin for the removal of diclofenac sodium (DS) from water. Sharper peaks of modified beads on spectrum of Fourier-transform infrared spectroscopy (FT-IR) revealed the successful synthesis with the introduction of more functional groups. It is remarkable that CS beads after grafting and crosslinking became more impenetrable to light and more stable. Regarding the surface of epichlorohydrin–polyethylenimine (EPCS@PEI), beads were rougher and smaller compared to unmodified CS beads, attributed to the presence of PEI. By comparison, CS beads grafted with glutaraldehyde and PEI grafted (GACS@PEI) were much smoother, which is connected to the lower adsorption capacity (Figure 1) [12].

Another work focused on tricaprylmethylammonium chloride CS hydrogel beads (CS-TCMA) for the fast adsorption of tetracycline (TC). TCMA has been demonstrated to enhance the adsorption capacity of TC, which is known as an ion-pairing reagent. The whole procedure, according to the research, lasts less than 45 min and has a 90% yield. This is very promising, considering the fact that tetracycline (TC) is the second-most produced and used antibiotic (cheap and high antimicrobial activity). Moreover, FTIR spectroscopy confirmed the incorporation of the TCMA on CS as well as the interaction between the hydrogel beads and the drugs. Scanning electron microscope (SEM) images reveal a dispersion of the TCMA on CS, concerning the homogenous porous structure of the composite [13].

2.2. Chitosan Nanoparticles/Chitosan Film

Many researchers have worked on chitosan nanoparticles, especially for drug delivery applications. However, another potential application is their use in water purification. In general terms, the techniques of preparation and the kind of cross-linking plays an important role to the properties of the final product. The research group of Riegger suggested emulsion cross-linking and described the impact of cross-linker concentration and the molecular weight of six commercial chitosans on chitosan nanoparticle formation. The best ratio found for glutaraldehyde: primary amino groups, in order to be narrowly distributed, covalent cross-linked, and form nanoscale chitosan particles, was found to be 1:1. Generally, covalent crosslinking is desired in the case of regeneration processes with strong pH changes, as the resulting products show a high chemical and thermal

stability. Prepared emulsions had an aqueous phase, chitosan solutions and an oil phase Span 80, and then NaCl was used to further stabilize the system (Figure 2). The adsorption behavior of the products was tested for two drugs: diclofenac (DCF) and carbamazepine (CBZ). Results from CBZ showed that untreated chitosans have lower adsorption than nanoparticles, while the lack of charge in CBZ is also associated with level of adsorption. In the case of DCF, there is the same tendency between the untreated chitosans and the nanoparticles. The study shows that smaller particles and better surface to volume ratio enhance the adsorption. For that reason, chitosan nanoparticles tend to have better results compared to untreated material. Broadly speaking, this system seems to be an interesting option for the treatment of drug-contaminated drinking water [14].

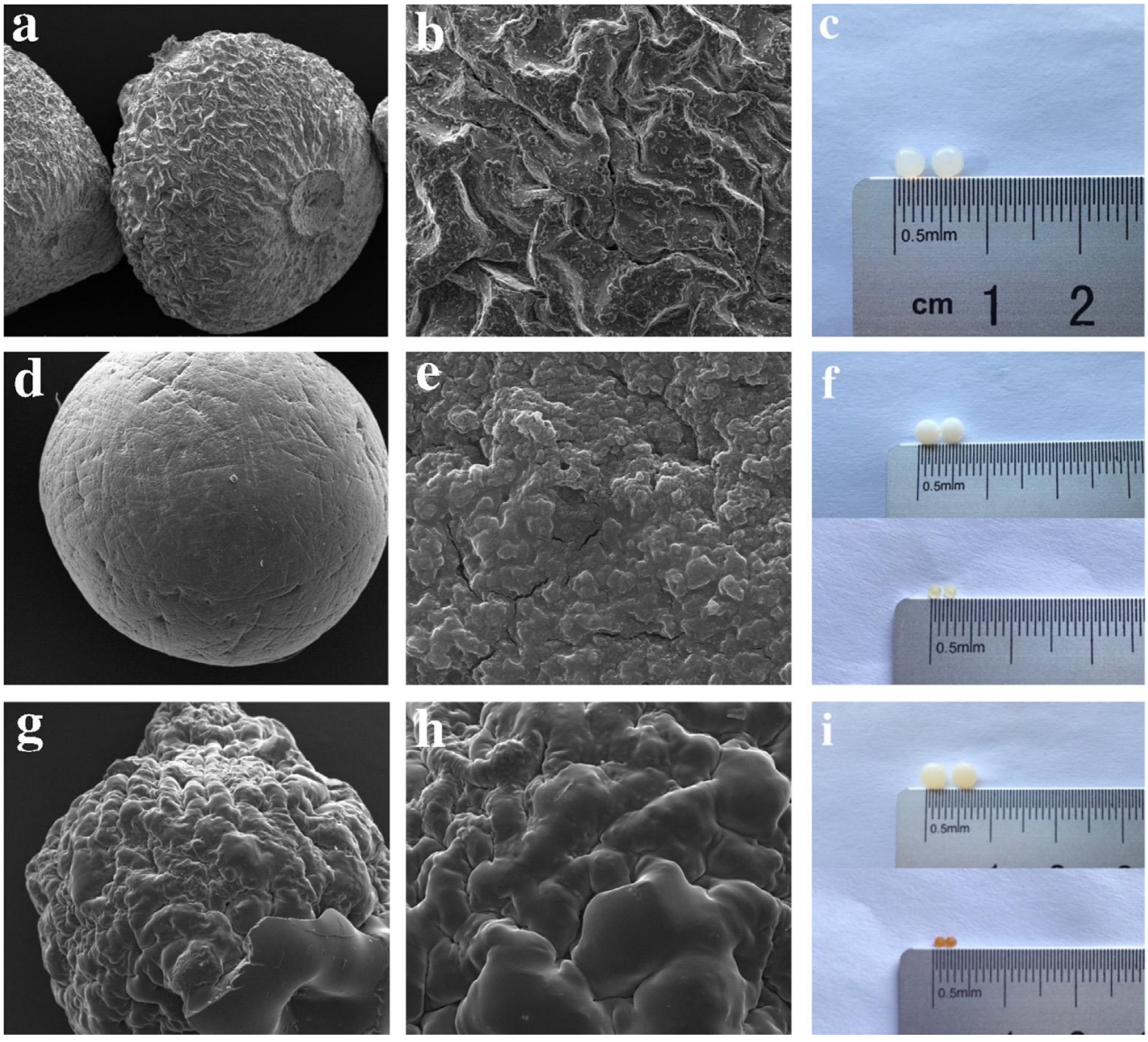

Figure 1. SEM images of (**a**,**b**) CS, (**d**,**e**) EPCS@PEI, (**g**,**h**) GACS@PEI beads. Photographs of wet and dried beads of (**c**) CS, (**f**) EPCS@PEI, and (**i**) GACS@PEI [12].

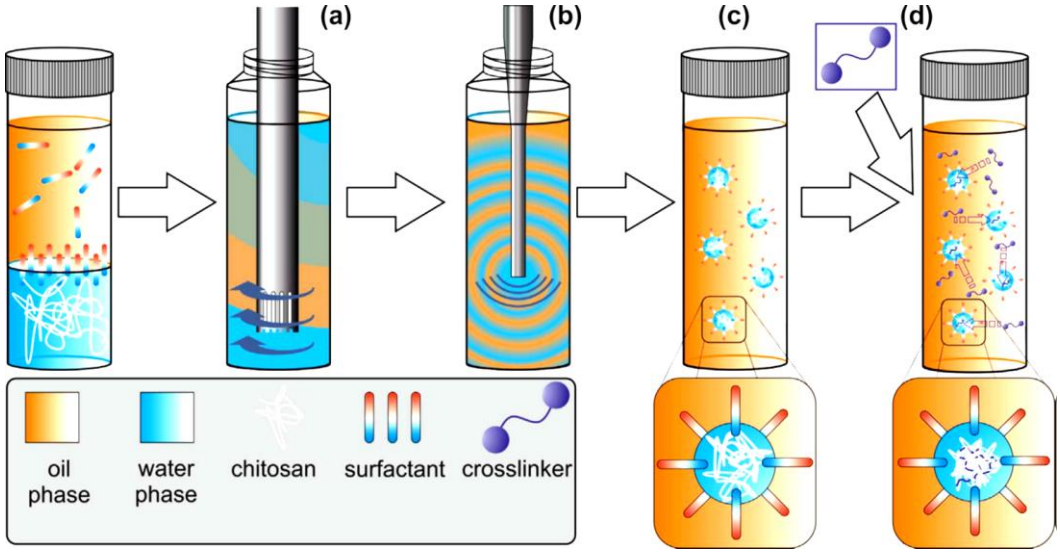

Figure 2. Schematical representation of emulsion crosslinking technique [14]. In a first step, the continuous phase was premixed with the disperse phase by rotor-stator treatment (**a**) followed by ultrasonication (**b**). To the resulting white and optically opaque emulsion (**c**) the crosslinker glut was added (**d**). To complete the crosslinking reaction, the emulsion was stirred for 18 h.

Rizzi et al. examined the removal of furosemide, one of the most dangerous pharmaceuticals, which causes hepatotoxicity and ototoxicity to aquatic species, from chitosan film. In addition, furosemide is associated with the development of toxic metabolites, even forced by its fractions. As a result, it is a challenge to find an adsorbent that is suitable for furosemide removal from waters and economically beneficial. Particularly, the adsorption was achieved due to interactions between the protonated amino groups of chitosan and the carboxyl groups of the drug molecule. A quite low adsorption capacity is presented (3.5 mg/g), with the aim of inorganic salt of sodium chloride (NaCl 1M) desorption of 90% of adsorbed furosemide performed, suggesting both the reuse of the pollutant and recycling of the adsorbent for more repetitions [15].

2.3. Grafted Chitosan

According to the fact that the adsorption of pharmaceuticals is depending also on the chemical structure of the biopolymer, it is of great importance to have enough sites available for chemical binding with the pollutants. This can happen with the grafting of chitosan and thus the introduction of extra functional groups. Kyzas et al. synthesized modified chitosan with sulfonic acid and cross-linked it with glutaraldehyde to examine the impact of humic acid in the whole process. Humic acid (HA) corresponds to the mixture of different acids and is a major compound of natural organic matter (NOM) and product of biodegradation of dead organic matter. As a model pharmaceutical pollutant, pramipexole dihydrochloride (PRM) was used. Drying method caused changes to the structure of the modified material, perhaps because of water molecules preexisting there. Broadly, the innovation of this study is supported by the coexistence of humic acid on the adsorbate pramipexole (PRM) in various concentrations. Results showed that the increase in the concentration of HA in water is associated with the decrease in the maximum adsorption capacity of pharmaceuticals, as there is a crucial concentration of HA at 5 mg/L. The same group also examined graphite oxide/poly(acrylic acid) grafted chitosan nanocomposite (GO/CSA) for its adsorption strength. FT-IR spectra showed that the existence of amino groups, because of basic conditions of preparation of the composite, can cause amine nucleophilic substitution on the epoxy groups of GO. The introduction of chitosan on GO cn be indicated by the absence of C=C absorbance due to the carbon structure network. The composite material appears more adsorption efficiency than neat graphite oxide or

poly(acrylic acid) grafted chitosan. Precisely, cationic groups of dorzolamide interacted with anionic groups of the derivatives while crosslinking with glutaraldehyde to increase the resistance in a wide range of pH. As a target drug, they used dorzolamide, a substance used for ocular release. It must be noted that the adsorption capacity was increased in a temperature range of 25–65 °C. It is remarkable that on FTIR spectroscopy of the adsorbent with dorzolamide, we can see the reduced peak of carbonyl groups of CSA and a new peak at 1622 cm^{-1}, which may be attributed to the amide I formation due to interactions between charged carboxyl groups of CSA and charged amino groups of the drug. There is a considerable literature from Kyzas' group on the subject, as they also studied modified chitosan with sulfonate (CsSLF) or N-(2-carboxybenzyl) groups (CsNCB) and crosslinked with glutaraldehyde in an effort to remove pramipexole dihydrochloride (PRM). It was found that alkaline conditions contribute to maximum adsorption while acidic conditions to maximum desorption. Results showed that modification enhanced the adsorption capacity while CsSLF present a better adsorption effect than CsNCB. The morphology of modified materials is not as smooth as the neat chitosan while CsSLF is rougher than CsNCB. The damage of the porosity of the material after modification showed affect the particle size of the materials/surface area. FTIR confirmed the modification although new peaks appeared due to the existence of homopolymers on the material. As a result, the two grafted materials are proposed as adsorbents with low cost and ecological perspective [16].

Another study from Tzereme et al. examined the adsorption capacity of four different grafted chitosans with succinic anhydride (CsSUC), maleic anhydride (CsMAL), itaconic acid (CsITA), and trans-aconitic acid (CsTACON) towards pharmaceutical compound diclofenac (DCF) and mixture of salicylic acid, ibuprofen, and ketoprofen. All materials were cross-linked with glutaraldehyde. The acidic condition of the process also facilitates the electrostatic attraction of cation amino groups of chitosan and negative carboxyl moieties of chitosan derivatives. In FTIR spectroscopy, new peaks appear at 1700–1740 cm^{-1} and also a lower intensity of $–NH_2$ peaks, facts that confirm the successful modification. Adsorption was carried out with several solvents [17].

Another research group used as an adsorbent modified chitosan with acrylic monomer, 2-(methacryloyloxy)ethyl dimethyl-(3-sulfopropyl)ammonium hydroxide in order to remove a mixture of anti-inflammatory drugs (diclofenac, ibuprofen, ketoprofen, paracetamol, and salicylic acid). The modification was prepared via free radical polymerization and the final material was further cross-linked with glutaraldehyde. Due to the coexistence of sulfonate anion groups and quaternary ammonium cations, the system interacts primarily with ionic forces and then with hydrogen bonds with the drug molecules. These interactions were also confirmed with FTIR spectroscopy. In conclusion, SEM images showed even smaller external pores than before adsorption.

2.4. Chitosan Composites with Magnetic Properties

Concerning the magnetic separation, this kind of separation is fast, expandable, easily automated, and can achieve complete separation compared to other techniques [18].

Ahamad and his group synthesized a new magnetic polymeric nanocomposite containing magnetic nanoparticles ($MnFe_3O_4$) (CDF@MF) and studied its application as adsorbent for tetracycline (TC). FT-IR study exhibited the successful synthesis of the composite material, concerning the characteristic absorption peaks. High surface area and favorable porous volume offers a promising substructure to the composite for more sites for adsorption. It seemed that CDF@MF had promising magnetic behavior that encourages the recyclability of the material after adsorption. Finally, SEM images showed the dispersion of the magnetic nanoparticles in the polymer matrix while the small size helps the adsorption of TC [19].

Zhang et al. referred to grafting co-polymerization on the surface of chitosan/Fe_3O_4 particles (CS-MCP). The aforementioned composite forms a core-brush structure, where the neat MCP constitute the core and the modified polymeric branches make up the brush layer. FT-IR measurements of the material demonstrated both $–NH_2$ and Fe-O absorptions. The modification was carried out to add functional groups to neat MCP

and thus help the adsorption process of organic pollutants. Diclofenac sodium (DCM) tetracycline hydrochloride was selected as an emerging organic contaminant. Enhanced removal capacity is due to the surface area available and core-brush topology and the interactions among positively charged polymeric branches and negatively charged groups of the pharmaceutical compounds (Figure 3) [20].

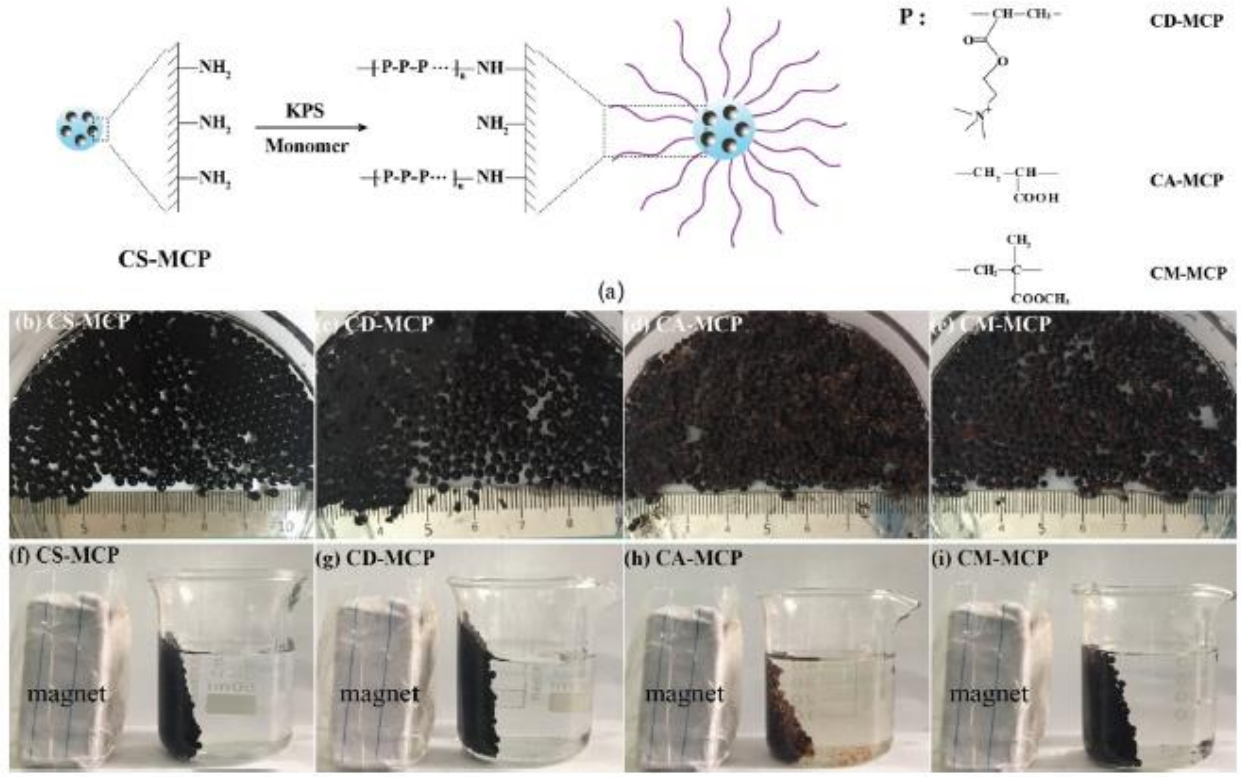

Figure 3. (**a**) Synthetic route, (**b**–**e**) photos, and (**f**–**i**) magnetic separation property of different adsorbents in water at room temperature [20].

Zhou et al. suggested core-brush structure containing chitosan and Fe_3O_4 composite particles (CS-MCPs) for the adsorption of commonly used norfloxacin (NOR), tylosin (TYL), and diclofenac sodium (DCF). They state that the most preferable process for the modification of MCP, in order to introduce extra functional groups, is a core of MCP and post-modification on the branches, which can easier contact the contaminant. FTIR spectra showed peaks at 1637 cm^{-1} and 609 cm^{-1}, referring to $–NH_2$ and Fe–O, respectively. In total, in this research, they tried to study the effect of brush modification of CS-MCP with polystyrene derivatives for the removal of pharmaceuticals. Concretely, modification with poly (sodium p-styrenesulfonate) enhanced the adsorption efficiency of NOR and TYL while modification with (poly-p-vinylbenzyl trimethylammonium chloride) successfully adsorbed DCF. In all cases, modification helped the pH resistance, in a narrow range of values, and also resulted in reusable systems (six cycles of processes). It is remarkable that after modification, the surface of CS-MCP becomes rough from smooth, and has better BET surface area. (Figure 4) [21].

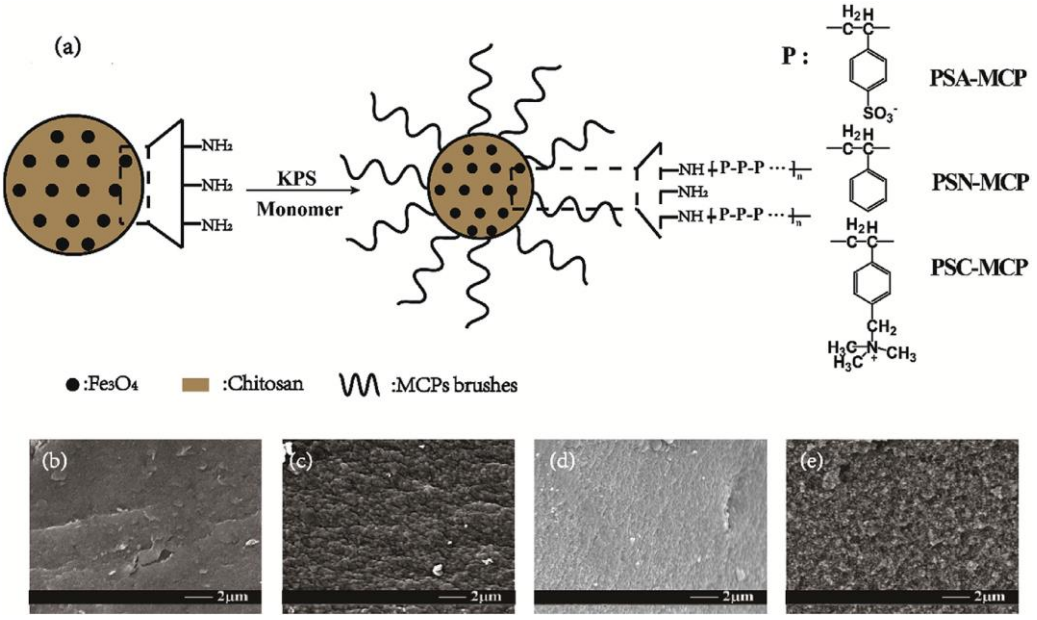

Figure 4. (**a**) Synthetic route; SEM images of (**b**) CS-MCP, (**c**) PSA-MCP, (**d**) PSN-MCP, and (**e**) PSC-MCP [21].

Liu used chitosan/graphene oxide-SO_3H composite (GC/MGO-SO_3H) with super paramagnetic behavior for the removal of ibuprofen and tetracycline. In the case of MGO-SO_3H, FTIR spectroscopy showed the characteristic peak of MGO-SO_3H at 560 cm^{-1}, while in the case of GC/MGO-SO_3H, hydrogen bonding between chitosan and GO is confirmed. The composite cross-linked with genipin for further stability. Chitosan magnetic composite has high congestion magnetization and magnetic permeability and graphene-based materials large surface area. In general, salts of chitosan magnetic composite could be merged with graphene oxide (GO) by electrostatic interaction. Precisely, the sulfa group is known to form stable complexes with various pharmaceuticals. Furthermore, the microporous structure with an ultra-large surface area enhanced the adsorption of ibuprofen and tetracycline drugs. The benefit of the hybrid is the ability to reuse it as it maintains the adsorption capacity at 85% after 5 cycles [22].

2.5. Chitosan Combined with MOFs

Another view of the subject gave Zhuo and his group using MOFs. In order to improve the ability of separation of neat metal organic frameworks (MOFs), they prepared MIL-101(Cr)/chitosan (MIL-101 (Cr)/CS) composite beads for the removal of ibuprofen (IBU) and ketoprofen (KET). A peak at 589 cm^{-1} on FTIR spectra prove the formation of the MOF, while the characteristic peaks of chitosan are shown, too. Compared to neat CS beads, the composite beads appear to have better adsorption capacity with a larger amount that can be withheld in the case of ketoprofen. Both element chromium (Cr) and protonated amino groups of chitosan help the conjunction with the pollutant, which was evaluated with X-ray photoelectron spectroscopy (XPS). Finally, the great regenerability composite beads appear, making them possible candidates for large-scale water treatment [23]. In another study, Jia et al. prepared a starch-chitosan-UiO-66-COOH composite as an adsorbent for pharmaceutical sulfonamide. Results showed hierarchical porosity of the composite and also efficient removal of the drug task. Chitosan seemed to facilitate the binding between starch and the MOF, proven also from FTIR spectra, and as well to decrease the aggregations of MOF nanoparticles during formulation. Zr-O bond of Zr-MOF with sulfonic groups of sulfonamide is the main reason of the efficient removal. The easy synthesis and the low cost are some advantages of the material [24].

2.6. Other Chitosan Composites

In the field of GO/CS composite, the research group of Delhiraja studied the composite material of activated carbon (AC), graphene oxide (GO), and chitosan (GO-AC-CS), combining the hydrophilicity, hydrophobicity, and binding properties of each component, respectively. A decrease in the intensity of transmittance in the carboxyl group region, in the case of GO-based composites, is connected to the new bond between the hydroxyl group of GO and the ring of chitosan. As pharmaceutical pollutants, they used acetaminophen (ACP) and carbamazepine (CBZ). The group took advantage of modified Hummer's method in order to obtain GO with many oxygen-containing functional groups. According to the results, the system shows a behavior sensitive to pH and organic matter. Concerning the morphology, SEM images showed clusters, flakes, and small ball-like formations for neat GO, AC, and CS, respectively. On the contrary, GO-CS appears as smooth clusters, confirming the bonding between the two. Figure 5 shows the insertion of chitosan between the crystal network of graphene oxide. Regeneration experiments showed that with appropriate organic solvent, the removal of the 80% of adsorbed matter can be achieved [25].

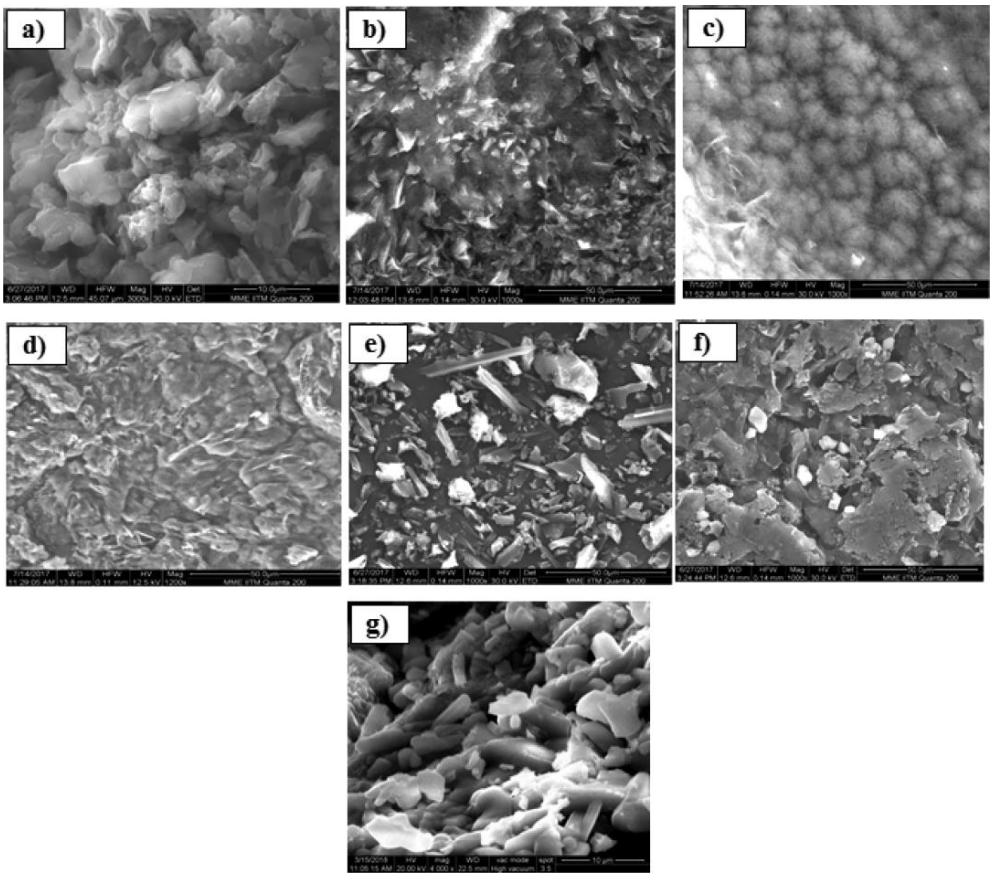

Figure 5. SEM images of the synthesized pristine and composite adsorbents (**a**) GO, (**b**) AC, (**c**) CS, (**d**) GO-CS, (**e**) AC-CS, (**f**) GO-AC-CS, and (**g**) cross-sectional SEM image of GO-AC-CS [25].

Other researchers examined the multifunctional combination of chitosan-EDTA-β-cyclodextrin (CS-ED-CD) for the deportation of ciprofloxacin, procaine, and imipramine from effluents. FTIR spectra of the composite showed new peaks compared to raw materials, due to carbonyl groups of amides formed and carboxylic groups inserted. The selection of EDTA as a cross-linker attracts interest because of its low cost and low toxicity compared to common cross-linkers. Likewise, chitosan contributes to higher loading of CD SEM images, indicating a thin, porous layer on the surface and a continuous porous internal morphology with pore sizes from 20 to 200 μm. Pore size measurements from SEM

and BET (Figure 6) are incompatible, but this a consequence of the different magnitude of dimensions in each method (pores sized less than 250 nm on BET and micrometers on SEM). As is expected on most biopolymers, the surface area and the porosity of the prepared complex were not notably higher, but that does not really influence the adsorption process, which mainly depends on the functional groups incorporated on the biopolymers [26].

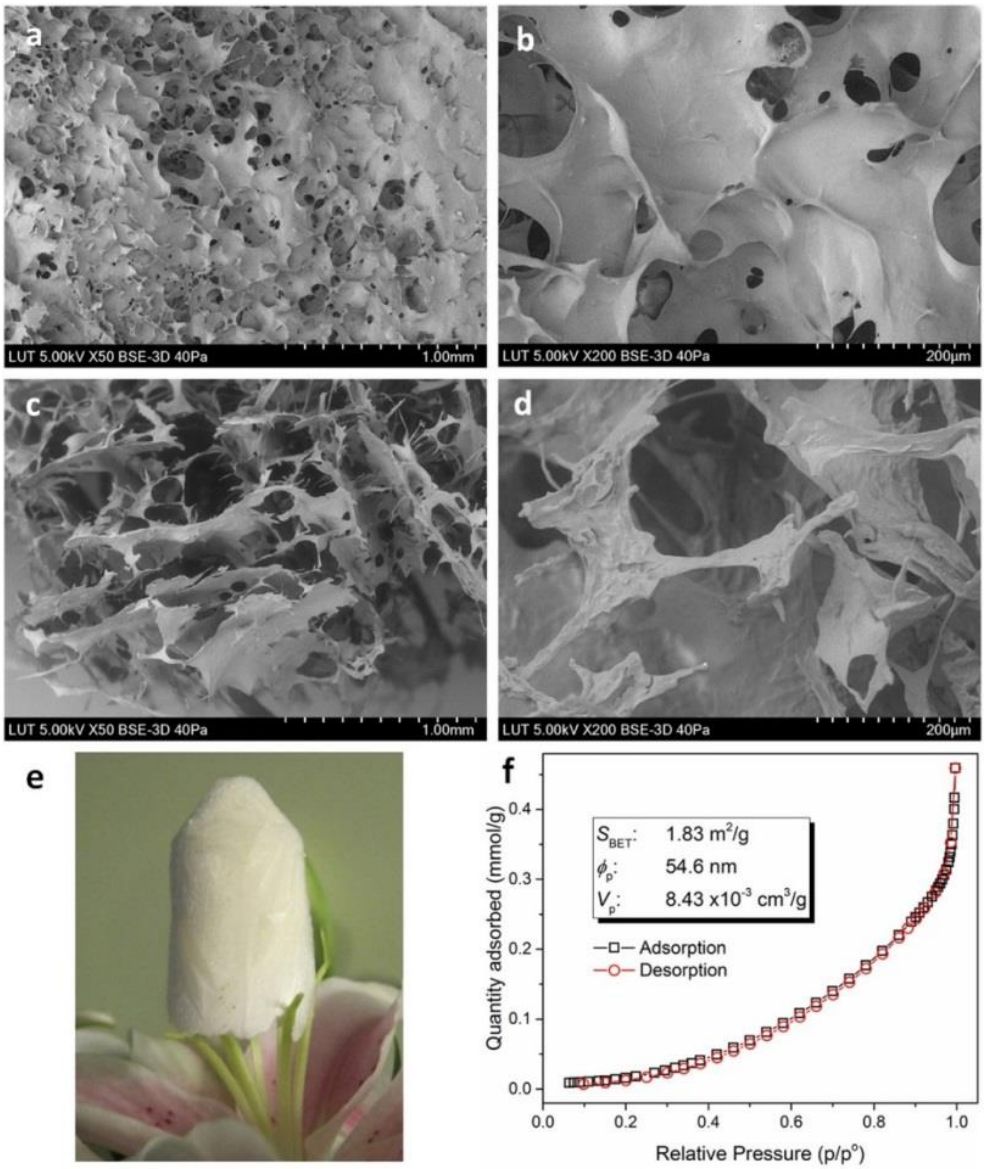

Figure 6. SEM images of freeze-dried CS-ED-CS polymer. Surface morphologies (**a**,**b**) and cross-sectional morphologies (**c**,**d**) of CS-ED-CD hydrogel with varying magnifications; a block of freeze-dried CS-ED-CD hydrogel standing on the stamens of a lilium flower (**e**); and BET isotherm linear plot and BET surface area (**f**), average pore diameter and cumulative pore volume data for CS-ED-CD [26].

Lessa et al., in order to adsorb from wastewaters metamizol (MET), acetylsalicylic acid (ASA), and acetaminophen (ACE) used a waste coffee grounds (WCG)-chitosan-poly (vinyl alcohol) (WCG-CA-PVA) composite. The concentration of 10% WCG in the system seems to be effective for the formulation, adding enough adsorption sites. SEM images indicate that increase in the WCG percentage provoke rougher surfaces and some aggregates, perhaps because there is a destruction of the compatibility of the polymer matrix and the filler. The main advantage of this research is the cost-beneficial process using the aforementioned waste and also the reusability in at least five cycles [27].

Regarding the important role of the size of the particles on adsorbent materials, Feng took advantage of the spray drying process in order to prepare, with a low cost, chitosan microparticles to acquire larger surface area. Particularly, he indicates the use of chitosan/nanographene oxide (CS/nGO) shows high adsorption efficiency of the anti-inflammatory drug diclofenac sodium (DCF). The 100% adsorption seems to be connected to coexisting hydrogen bonding and the electrostatic interactions among the positive charged amino groups and the anions of the compounds. They presented that the addition of nGO promote the reusability of the microspheres with 80% capacity of adsorption of DCF after six cycles of action [28]. With the same concept as Feng, Yanyan et al. investigated, among others, the use of modified multi-walled carbon nanotubes (MWCNTs) with chitosan coating for the adsorption of acetaminophen (Ace) from wastewater, in order to ameliorate the attachment of the model drug. It seems that chitosan coating in MWCNT also filled the interval between nanotubes. Specifically, in the case of chitosan coated MWCNTs, a new peak at 1630 cm^{-1} seems to reveal the presence of chitosan. Nevertheless, the treatment of MWCNT with ozone seems to be more efficient for the adsorption of acetaminophen, perhaps due to the presence of extra hydroxyl and carboxyl groups. At the same time, even more bioprocesses are required to achieve the limit of less than 0.2 mg/L, as reported by Chinese regulations [29].

3. Adsorption Evaluation

3.1. Isotherm Models and Kinetic Equations

In this study, regarding the use of nanoadsorbents, some theoretical equations (models) are presented, explained, and analyzed. In addition, according to those theoretical equations, some crucial adsorption parameters are evaluated. The parameters include the adsorption capacity and kinetic rate.

3.1.1. Isotherm Models

In order to analyze innovative adsorbents, the selection of the most appropriate adsorption equilibrium correlation is important for the selection of the ideal adsorption system. The isotherms of adsorption, which are commonly named as equilibrium equations, are essential in order to optimize the mechanism paths of adsorption, expression of capacities, and surface properties of adsorbents, and also to ensure the productive design of the systems of adsorption since they explain how the model pollutants are interrelated with the materials of adsorption process (adsorbent).

The phenomenon can be explained via the mobility or release of a substance from the aquatic environments or aqueous porous media to a solid-phase at a persistent pH and temperature, in broad-spectrum. Consequently, the obtained isotherm of adsorption is an invaluable curve. The plotting graph between residual concentration and solid-phase normally represents the mathematical association towards the operational design, modeling analysis, and applicable practice of the systems of adsorption.

In the case where the solute concentration remains stable or unchanged due to zero net transfer of solute adsorbed and desorbed from the surface of adsorbent, the phase of equilibrium is achieved. However, the concentration of equilibrium of the adsorbate in the liquid and solid phase at a predefined temperature can be indicated by the sorption isotherms of equilibrium phase. The shapes of isotherms that can be formed include strongly favorable, favorable, unfavorable, linear, and irreversible types. In addition, a variety of equilibrium isotherm models (Langmuir, Freundlich, Langmuir–Freundlich, Brunauer–Emmett–Teller (BET), Dubinin–Radushkevich, Redlich–Peterson, Temkin, Toth, Koble–Corrigan, Sips, Khan, Hill (FHH), Flory–Huggins, Radke–Prausnitz, MacMillan–Teller (MET) isotherm), have been developed [30]. The model pollutant's amount which is removed until the achievement of the phase of equilibrium Q_e (mg/g) is calculated according to the equation of mass balance and given by:

$$Q_e = \frac{(C_0 - C_e)V}{m} \quad (1)$$

where C_0 and C_e (mg/L) are the initial and equilibrium concentration of model pollutants, respectively; V (L) and m (g) are the volume of adsorbate (solution) and the mass of adsorbent, respectively.

3.1.2. Kinetic Equations

Kinetic studies are important in order to predict the optimal conditions of the processes. Kinetic modelling provides details about the mechanism of adsorption and possible steps of rate-controlling, such as the processes of chemical reactions or mass transport. In addition, several models of kinetics have been developed but the most prevalent ones are the pseudo-first order and pseudo-second order equations. Moreover, there are other kinetic equations that are not extensively used, such as Elovich, and intra-particle diffusion [30].

3.2. Discussion

Below, several selected studies for the removal of pharmaceuticals (Table 1) from synthetic aqueous solutions by using chitosan-based composite adsorbents are presented. The optimal value of pH and best mathematical fitting of isotherms models and kinetics equations are also shown, as well as the adsorption capacity (Q_{max}) of the selected chitosan-based composite adsorbents. The isotherm models used are Langmuir (L), Freundlich (F), Langmuir–Freundlich (L–F), Temkin (T), Dubinin–Radushkevich (D–R) and Sips (S). Finally, the kinetic equations used are pseudo-first order (PFO), pseudo-second order (PSO), intra-particle diffusion (I-PD), and Elovich (ELV).

Table 1. Selected studies for the adsorption of pharmaceutical compounds from aqueous solutions at 25 °C using modified chitosan adsorbents. The optimum mathematical fitting of isotherm and kinetic models, derived from the experimental results after the adsorption process, are abbreviated with parenthesis.

Sorbent	pH	Pharmaceutical	Isotherms	Kinetics	Q_{max} (mg/g)	Ref.
$MnFe_2O_4$ nanoparticles embedded chitosan-diphenylureaformaldehyde Resin (CDF@MF)	6	Tetracycline	(L), F, T	(PFO), PSO, I-PD	168.24	[19]
Ionic liquid-impregnated chitosan hydrogel beads (CS-TCMA)	7		(L), F, S	(PFO), PSO, I-PD	17.15	[13]
Chitosan/Fe_3O_4 composite particles (CD-MCP)	10		(L), F, D–R	PFO, (PSO), I-PD, ELV	50.1	[20]
Genipin-crosslinked chitosan/graphene oxide-SO_3H (GC/MGO-SO_3H)	7		(L), F	PFO, (PSO)	473.28	[22]
Chitosan/Fe_3O_4 composite particles (CD-MCP)	6	Diclofenac	(L), F, D–R	PFO, (PSO), I-PD, ELV	196	[20]
Magnetic composite particle (MCP) adsorbent, Core-brush shaped chitosan-based MCPs with core-brushes of polyanions (poly(sodium p-styrenesulfonate)) (PSA-MCP)	6		L, F, (T)	PFO, (PSO)	151	[21]
Chitosan grafted with trans-aconitic acid (CsTACON)	4		L, F, (L–F)	PFO, (PSO)	84.56	[17]
Epichlorohydrin-polyethylenimine adsorbent (EPCS@PEI)	5		(L), F	PFO, (PSO)	253.32	[12]
Chitosan microspheres with nanographene oxide	—		F	PFO, (PSO)	20	[28]
Graphite oxide/poly(acrylic acid) grafted chitosan nanocomposite (GO/CSA)	3	Dorzolamide	L, (L–F)	PSO	334	[31]
Sulfonate-grafted chitosan adsorbent (CsSLF)	10	Pramipexole	L–F	PFO, (PSO), ELV	337	[32]
N-(2-carboxybenzyl)-grafted chitosan adsorbent (CsNCB)	10		L–F	PFO, (PSO), ELV	181	[32]
Sulfonic acid-grafted chitosan adsorbent (CsSLA)	10		L, (L–F)	Not presented	339	[16]
Magnetic composite Particle, Core-brush shaped chitosan-based MCPs with core-brushes of polyanions (poly(sodium p-styrenesulfonate))	3	Norfloxacin	L, F, (T)	PFO, (PSO)	165	[21]
Magnetic composite Particle, Core-brush shaped chitosan-based MCPs with core-brushes of polyanions (poly(sodium p-styrenesulfonate))	4	Tylosin	L, F, (T)	(PFO), PSO	134	[21]
Chitosan/waste coffee grounds	6	Metamizol	L, (F), T, D–R	PFO, (PSO), ELV, I-PD	6.29	[27]

Table 1. *Cont.*

Sorbent	pH	Pharmaceutical	Isotherms	Kinetics	Q_{max} (mg/g)	Ref.
Chitosan/waste coffee grounds	6	Caffeine	L, (F), T, D–R	PFO, (PSO), ELV, I-PD	8.21	[27]
Chitosan/waste coffee grounds	6	Acetaminophen	L, (F), T, D–R	PFO, (PSO), ELV, I-PD	7.52	[27]
Chitosan/waste coffee grounds	6	Acetylsalicylic acid	L, (F), T, D–R	PFO, (PSO), ELV, I-PD	9.92	[27]
Ozone-treated MWCNTs	4		L, (F)	PFO, (PSO)	205	[29]
Graphene oxide-activated carbon-chitosan composite (GO-AC-CS)	7		(L), F	PFO, (PSO)	13.7	[25]
Graphene oxide-activated carbon-chitosan composite (GO-AC-CS)	4	Carbamazepine	(L), F	PFO, (PSO)	11.2	[25]
Chitosan grafted carboxylic Zr-MOF to porous starch (PS-chitosan-UiO-66-COOH)	3	Sulfanilamide	(L), F	PFO, (PSO), I-PD	70.20	[24]
Chitosan film	5–6	Furosemide	(L), F, T, D–R	PFO, (PSO)	3.5	[15]

3.2.1. Pharmaceutical Compounds—Effect of pH

A crucial parameter for the effectiveness of the adsorption process is the value of pH. In the study of Yangshuo Liu et al., the maximum removal efficiency of tetracycline (TC), for GC/MGO-SO_3H (473.25 mg/g), was achieved at pH 10, while at higher pH values the removal efficiency slightly decreased. This fact is attributed to the surface of GO, which gains functional groups with negative charge, after the pH increase, resulting in an enhanced ionic interaction for the binding of tetracycline molecules on the surface of composite adsorbent in aqueous solutions. In the case of very high values of pH, electrostatic repulsion occurs between charges, resulting in the lower binding of tetracycline molecules [22]. However, in the study of Ahamad et al., the maximum removal efficiency, for CDF@MF (168.42 mg/g), was achieved at pH 6. Consequently, the acidic sites make the process of adsorption favorable because they can donate protons depending on the pH of the synthesized aqueous solution. From the values of the zeta potential of synthesized composite adsorbent in TC solution is revealed that there is an interaction of π-π stacking energy between the surface of synthesized composite adsorbent and TC in aqueous solution. At pH values higher than 6 (Figure 7), electrostatic repulsion occurs, resulting in the lower binding of TC molecules and consequently a lower adsorption efficiency [19]. Thus, a general result can be concluded that according to the composite adsorbent used, the pH of the synthesized aqueous solution should be carefully adjusted in an appropriate way in order to avoid the electrostatic repulsions between charges.

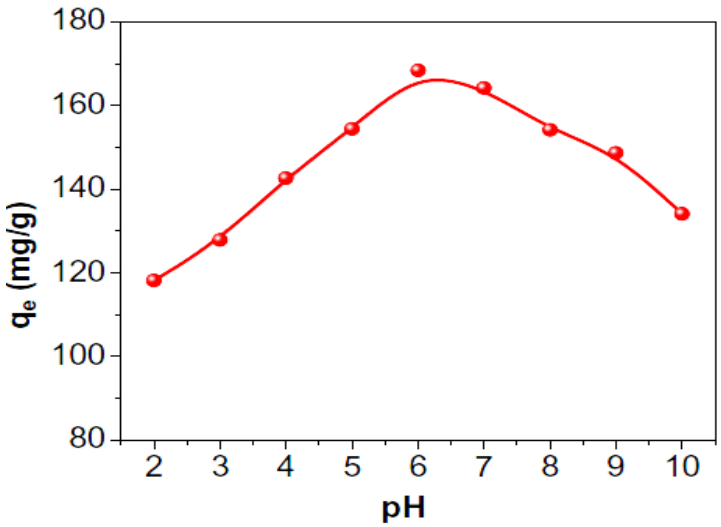

Figure 7. pH effect for the removal of TC from aqueous solution by using CDF@MF composite adsorbent [19].

In terms of diclofenac removal from aqueous solution, we take a look at the following experimental studies. In the study of Yuqing Lu et al., the maximum removal efficiency of diclofenac (DCF), for EPCS@PEI (253.32 mg/g), was achieved at pH 5. For pH values higher

than 4.2, DCF molecules charged with negative value result in the strong attraction of DCF molecules onto the surface of synthesized composite adsorbent due to its ammonium functional groups. In addition, the obtained adsorption capacity and zeta potential of the EPCS@PEI reached values of pH 4.2–9.0. In addition, with the increase in pH value from 4.2 to 7.0, a decrease in zeta potential is observed, and thereafter a slight increase when the pH value increases to 9.0. This result points out the protonation of amino groups at low values of pH. The adsorption capacity and its increasing trend is in agreement with the values of zeta potential. Moreover, the optimum pH 5 was selected because at pH ~4.2, precipitation of DCF occurs. In addition, at the optimum value of pH, the amine groups are protonated on the surface of the composite adsorbent and generate positive-negative charges, which greatly promote the adsorption of DCF on beads of EPCS@PEI. It must be noted that the DCF model pollutant was effectively removed on beads of EPCS@PEI at all examined values of pH (4.2–9.0). Consequently, the selected cross-linking agent for the EPCS@PEI beads adsorbent was epichlorohydrin [12].

In another study by Shaopeng Zhang et al., the maximum removal efficiency of diclofenac (DCF), for CD-MCP (196 mg/g), was achieved at pH 6. They concluded that the optimum value of pH occurs when the predominant species are the anions of DCF pharmaceutical. The main interactions during the process of adsorption is charge attraction, because CD-MCP has strong cationic functional groups. When the value of pH falls below the optimum value, cations or neutral molecules of the DCF model pollutant are not favored for the composite adsorbent with a positively charged surface. However, in the case where the value of pH passes the optimum value, more anions of hydroxyls in water solution generate a competitive effect with the anions of DCF pharmaceutical, resulting the decrease in adsorption capacity. More specifically, the effect of competitivity between DCF and OH^- can also indicate why the optimal q_{max} for the removal of DCF from aqueous solution is so high. In general, it can be concluded that DCF removal occurs at optimum pH 6 due to the trace availability of OH^- group [20].

In the study of Kyzas et al., the maximum removal efficiency of pramipexole (PRM) for CsSLF (307.18 mg/g) was achieved at pH 10. In addition, with the increasing of solution pH (2–12), the anionically grafted derivatives are deprotonated, resulting in the generation of strong attractive forces between the grafted chitosan material (negatively charged) and PRM molecule (positive charged), which resulted in high values of removal (%). The interactions between the CsSLF and PRM molecule at pH 10 [32] are presented in Figure 14.

3.2.2. Pharmaceutical Compounds—Evaluation of Adsorption Isotherm Models

The isotherm models, which were selected for the determination of appropriate isotherm for the uptake of TC on GC/MGO-SO_3H, were L and F. From the isotherm models used it was concluded that the model of L fits better to the experimental data when compared with the model of F, implying monolayer coverage of TC on the surface of GC/MGO-SO_3H, and also indicates active sites with homogeneous distribution on the surface of the adsorbent. In addition, the value of 1/n of TC on the GC/MGO-SO_3H was 0.2530, indicating that the TC model pollutant can easily be adsorbed on the surface of GC/MGO-SO_3H [22]. In addition, in the case of CDF@MF for the removal of TC from aqueous solution, the isotherm models of L, F, and T (Figure 8) were selected. According to the values of R^2, the TC adsorption on the surface of CDF@MF supports the isotherm model of L. More specifically, the values of the correlation coefficient (R^2) in the case of L, F, and T isotherm models were 0.9955, 0.9632, and 0.9210, respectively. However, the value of $Q_{max,cal}$ according to the calculation from the model of L is in accordance with the value of $q_{max,exp}$ derived from the experimental process [19].

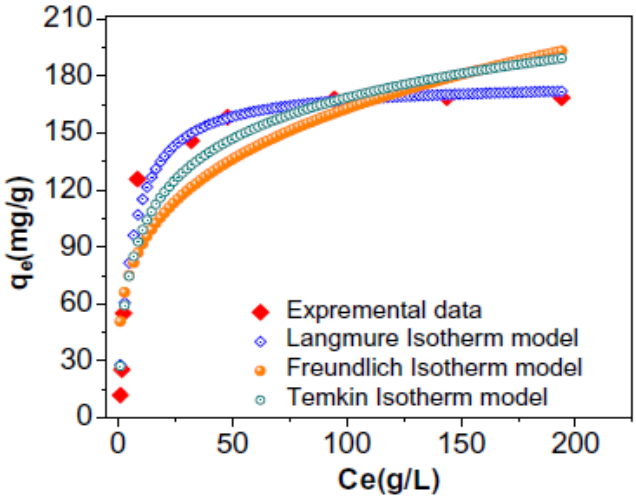

Figure 8. Adsorption isotherm of TC on CDF@MF [19].

Thereafter, for the removal of DCF from aqueous solution by using the EPCS@PEI adsorbent, the isotherm models of L and F were selected. The model of L presents larger values of R^2 when compared with the model of F, indicating a better mathematical fitting to the experimental data. It was also found that the root mean squared error (RMSE) value for the adsorption isotherm model of L was smaller when compared with the value of F adsorption isotherm (298 K). Thus, it can be concluded that the process of adsorption can be described effectively by using the model of L, indicating monolayer adsorption of DCF on the surface of EPCS@PEI adsorbent [12].

In addition, in the case of CD-MCP for the removal of DCF from aqueous solution, the isotherm models of L, F, and D–R were selected. According to the value of R^2, it was found that the model of L has better mathematical fit to the experimental data, indicating monolayer coverage of DCF onto the (poly(2-methyl acryloyloxyethyl trimethyl ammonium chloride), PDMC) brushes of CD-MCP adsorbent [20].

Finally, according to the selected adsorbent materials, in the case of PRM removal from aqueous solution, by using the CsSLF adsorbent, the isotherm model of L–F (Figure 15) was selected, which has a successful mathematical fitting to the isotherm model of L–F (R^2 = 0.99). It must be noted that CsSLF adsorbent can easily interact with amino groups (primary and secondary) [32].

3.2.3. Pharmaceutical Compounds—Adsorption Kinetics

The adsorption kinetics of TC, by using the GC/MGO-SO_3H adsorbent, were investigated in order to verify the mechanism of adsorption. According to the highest correlation coefficient (R^2 = 0.9983), the adsorption of TC on the surface of GC/MGO-SO_3H has better mathematical fitting to the PSO kinetic equation. The value of $Q_{e,cal}$ for the adsorption of TC model pollutant was in very close accordance with the value of $Q_{e,exp}$, in the case of PSO kinetics [22]. Moreover, the adsorption kinetics of TC, by using the CDF@MF adsorbent, were investigated in order to verify the mechanism of adsorption. According to the highest correlation coefficient (R^2 = 0.9961), the adsorption of TC on the surface of CDF@MF has better mathematical fitting to the PFO kinetic equation. In addition, the $Q_{e,cal}$ (170.20 mg/g) for the adsorption of TC model pollutant were in very close accordance with the value of $Q_{e,exp}$ (168.42 mg/g), in the case of PFO kinetics, indicating a physio-adsorption process [19].

Moreover, the adsorption kinetics of DCF, by using the EPCS@PEI adsorbent, were investigated in order to verify the mechanism of adsorption. In addition, according to the highest correlation coefficient (R^2 = 0.9686), the adsorption of DCF on the surface of EPCS@PEI has better mathematical fitting to the PSO kinetic equation, when compared with the PFO kinetic equation (R^2 = 0.9579), indicating a chemisorption process. Moreover,

the values of RMSE in the case of PFO kinetics were bigger when compared with those of PSO kinetics [12]. In addition, the adsorption kinetics of DCF, by using the CD-MCP adsorbent, were investigated in order to verify the mechanism of adsorption. The high value of R^2 in the case of PSO demonstrates that this model represents the data of kinetics, and also indicates a chemisorption process between adsorbent and adsorbate. This result is in accordance with previous deductions that charge attraction among the PDMC brushes of quaternary ammonium groups, and the anions of model pollutant. Furthermore, according to the equation of Arrhenius, it was found that the adsorption activation energy (E_a) was 12.85 kJ/mol [20].

Finally, the adsorption kinetics of PRM, by using the CsSLF adsorbent, were investigated in order to verify the mechanism of adsorption. The high value of R^2 in the case of PSO model (R^2 = 0.977) demonstrates that this model represents the data of kinetics, and also indicates a chemisorption process between adsorbent and adsorbate. Moreover, it must be noted that the calculated value of $Q_{e,cal}$ is in accordance with the data $Q_{e,exp}$, a result that indicates that the system of adsorption belongs to the kinetic model of PSO equation [32].

3.3. Personal Care Products

Presented below several selected studies for the removal of personal care products (Table 2) from synthetic aqueous solutions by using chitosan-based composite adsorbents. Also presented are the optimal values of pH, the preferred and best mathematical fitting of isotherms models and kinetics equations, and also the adsorption capacity (q_{max}), of the selected chitosan-based composite adsorbents. The isotherm models used are L, F, L–F, and Redlich–Peterson (R–P). Finally, the kinetic equations used are PFO, PSO, and I-PD.

Table 2. Selected studies for the adsorption of personal care products from aqueous solutions, at 25 °C using modified chitosan adsorbents. The optimum mathematical fitting of isotherm and kinetic models, derived from the experimental results after the adsorption process, are abbreviated with parenthesis.

Sorbent	pH	Pollutant	Isotherms	Kinetics	Q_{max} (mg/g)	Ref.
Graphene oxide-activated carbon-chitosan composite (GO-AC-CS)	4	Bisphenol A	(L), F	PFO, (PSO)	13.2	[25]
	7	Caffeine	(L), F	PFO, (PSO)	14.8	[25]
	4	Triclosan	(L), F	PFO, (PSO)	14.5	[25]
Genipin-crosslinked chitosan/graphene oxide-SO_3H (GC/MGO-SO_3H)	6	Ibuprofen	(L), F	PFO, (PSO)	113.27	[22]
MIL-101(Cr)/chitosan composite beads	4	Ibuprofen	L, F, (R–P)	PFO, (PSO), I-PD	103.2	[23]
		Benzoin acid	L, F, (R–P)	PFO, (PSO), I-PD	66.5	[23]
		Ketoprofen	L, F, (R–P)	PFO, (PSO), I-PD	156.5	[23]
Bio-derived chitosan-EDTA-β-cyclodextrin(CS-ED-CD)	4	Bisphenol S	L, (L–F)	PSO	44.3	[26]
	4	Ciprofloxacin	L, (L–F)	PSO	47.1	[26]
	5	Procaine	L, (L–F)	PSO	48	[26]
	5	Imipramine	L, (L–F)	PSO	41.8	[26]

3.3.1. Personal Care Compounds—pH Effect

In the study of Krithika Delhiraja et al., the maximum removal efficiency of bisphenol A (BPA), for GO-AC-CS (13.2 mg/g), was achieved at pH 4.0–6.0, while at higher pH values (7.0–12.0), the removal efficiency decreased, which is attributed to the surface

deprotonation of functional groups. It must be noted that the BPA compound under the pH value of 8 exists in its neutral form, but with the pH increase above 8 is deprotonated to an anionic form. Consequently, at high value of pH occurs electrostatic repulsion between the negatively charged surface of GO-AC-CS and anionic BPA, resulting in the decrease in removal efficiency. In addition, the removal efficiency of caffeine (CAFF) revealed increase uptake in the case of neutral pH, and thereafter, efficiency of uptake decreased in the case of high pH due to the hydrophilic nature of the compound. The adsorption efficiency of triclosan (TCS), similar to BPA, found to be increasing in the case of low pH (pH 4). In addition, it was concluded that the main driving forces for the sorption of TCS on the surface of the GO-AC-CS were hydrogen bonding, π-π and hydrophobic interactions. The increased value of pH and the decrease in the adsorption of TCS is attributed to the electrostatic repulsion between the negatively charged surface of GO-AC-CS and anions of TCS. Previously studies have shown higher uptake of TCS from aqueous solution at low values of pH. So, according to this study, it can be concluded that the uptake of model pollutants was based on the value of pH and for this reason needs to be optimized prior the adsorption process [25].

In the study of Yangshuo Liu et al., the maximum removal efficiency of ibuprofen (IBU), for GC/MGO-SO_3H (113.27 mg/g), was achieved at pH 6. The pH effect was examined for the adsorption of IBU at the pH value 2–12, using acid/base buffer solutions. With the increase in pH from 2 to 6, the removal increases from 65.42 to 122.35 mg/g. Moreover, with the increase in pH higher than 6, the IBU compound obtains a negative charge, resulting in the decrease in adsorption capacity because these negative charges may possibly be involved in electrostatic interactions with the surrounding ions of IBU that became stronger when pH increased [22].

3.3.2. Personal Care Products—Evaluation of Adsorption Isotherm Models

The isotherm models selected for the determination of appropriate isotherm for the uptake of BPA, CAFF, and TCS on GO-AC-CS were L and F (Figure 9). From the isotherm models used, it was concluded that the model of L fits better to the experimental data, when compared with the model of F, implying monolayer coverage of BPA, CAFF, and TCS on the surface of GO-AC-CS, and also indicating active sites with homogeneous distribution on the surface of adsorbent. More specifically, the R^2 values of the L model for BPA, CAFF, and TCS were 0.988, 0.970, and 0.992, respectively, while those of the F model were 0.983, 0.964, and 0.949, respectively. However, at the phase of equilibrium, the adsorbed amounts on the surface of GO-AC-CS were in order of CAFF > TCS > BPA. In addition, the obtained R_L value after the calculation of the spontaneous nature of the adsorption process was between 0 and 1, revealing that the process of adsorption is highly spontaneous or favorable. Through the isotherm model F, it was found that the constant (1/n) takes values less than 1, in all cases, which indicates a higher degree of bonding between adsorbent and adsorbate [25].

In addition, the isotherm models that were selected for the determination of the appropriate isotherm for the uptake of IBU on GC/MGO-SO_3H were L and F. From the isotherm models used it, was concluded that the model of L fits better to the experimental data, when compared with the model of F, implying monolayer coverage of IBU on the surface of GC/MGO-SO_3H, and also indicates active sites with homogeneous distribution on the surface of adsorbent. In addition, the value of 1/n of IBU on the GC/MGO-SO_3H was 0.2414, indicating that the IBU model pollutant can be easily adsorbed on the surface of GC/MGO-SO_3H (Table 3) [22].

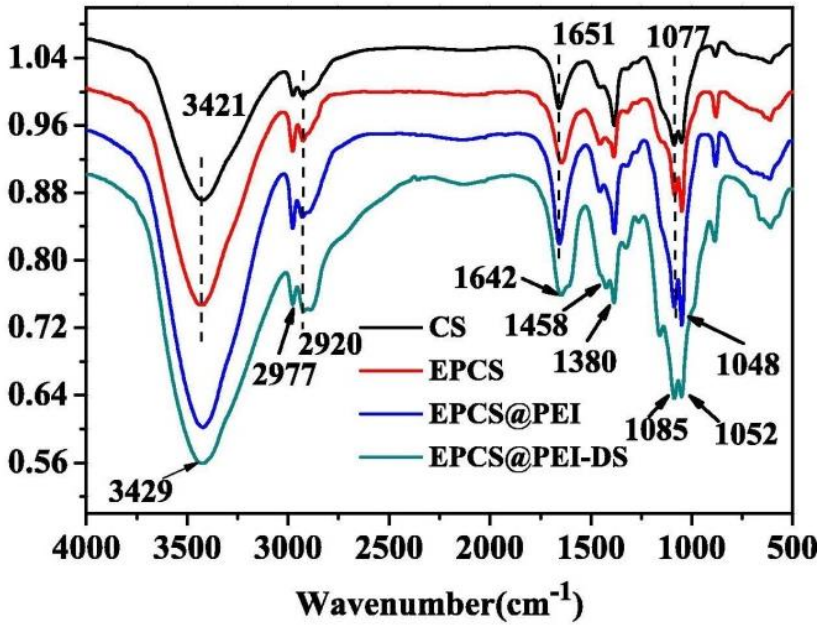

Figure 9. FTIR spectra of CS, EPCS, and EPCS@PEI before and after adsorption (in the above Figure, DS is abbreviated the DCF compound) [12].

Table 3. Parameters for the calculation of L and F models [22].

Pharmaceutical	T	Langmuir				Freundlich		
	K	K_L	Q_{max} (mg/g)	R^2	K_F	1/n	R^2
IBU	298	2.017	138.62	0.9999	5.46	1.2530	0.9122
	308	2.236	160.83	0.9992	6.35	1.1263	0.8247
	313	1.865	146.27	0.9978	5.68	1.2724	0.7893

3.3.3. Personal Care Products—Adsorption Kinetics

The adsorption kinetics of BPA, CAFF, and TCS, by using the GO-AC-CS adsorbent, were investigated in order to verify the mechanism of adsorption. As it can be observed in Table 4, the highest correlation coefficient values (R^2 = 0.999), which were achieved for the adsorption of BPA, CAFF, and TCS on the surface of GO-AC-CS, were obtained with the PSO kinetic model. Moreover, the $Q_{e,exp}$ and $Q_{e,cal}$ values of the PSO kinetic model was almost equal, indicating a chemisorption process via electrostatic forces, where the exchange or sharing of electrons occurs between the ionized adsorbate species and GO-AC-CS composite adsorbent [25].

Table 4. PFO and PSO kinetic parameters for the adsorption of BPA, CAFF, and TCS personal care products from aqueous solutions, over GO-AC-CS composite adsorbents [25].

Compound	Adsorbent	Capacity	PFO			PSO		
		Q_{max} (mg/g)	k_1 (h^{-1})	$q_{e,cal}$ (mg/g)	R^2	k_2 (g/mg/h)	$q_{e,cal}$ (mg/g)	R^2
BPA	GO-AC-CS	18.4 ± 0.55	0.527	14.2	0.976	0.04	30.3	0.999
CAFF	GO-AC-CS	19.8 ± 0.11	0.374	3.99	0.824	0.487	19.7	0.999
TCS	GO-AC-CS	19.5 ± 0.95	0.587	4.51	0.904	0.65	19.6	0.999

The adsorption kinetics of IBU, by using the GC/MGO-SO_3H adsorbent, were investigated in order to verify the mechanism of adsorption. According to the high R^2 = 0.99, the uptake of IBU can be successfully described by the PSO model. The value of $Q_{e,cal}$ for the

adsorption of IBU model pollutant was in very close accordance with the value of $Q_{e,exp}$, in the case of PSO kinetics [22].

3.4. FTIR Analysis for Adsorption Mechanism

It can be clearly observed that after the adsorption of DCF using EPCS@PEI beads, changes are presented in the range of 1700–1000 cm^{-1}. More specifically, the peaks located approximately at 1651 cm^{-1}, 1077 cm^{-1}, and 1048 cm^{-1} shifted to 1642 cm^{-1}, 1085 cm^{-1}, and 1052 cm^{-1}, respectively, after DCF adsorption onto EPCS@PEI beads, while the broad band at 3421 cm^{-1} shifted to 3429 cm^{-1} (Figure 9) [12]. In another study by Sara Ranjbari et al., after the adsorption of TC onto CS-TCMA, there was a considerable red shift at C=O stretching the vibration from 1646 cm^{-1} to 1626 cm^{-1}, indicating the interaction of the CS structure with TC molecules. The structural reaction between CS-TCMA adsorbent composite and TC molecules is presented in Figure 10 [13].

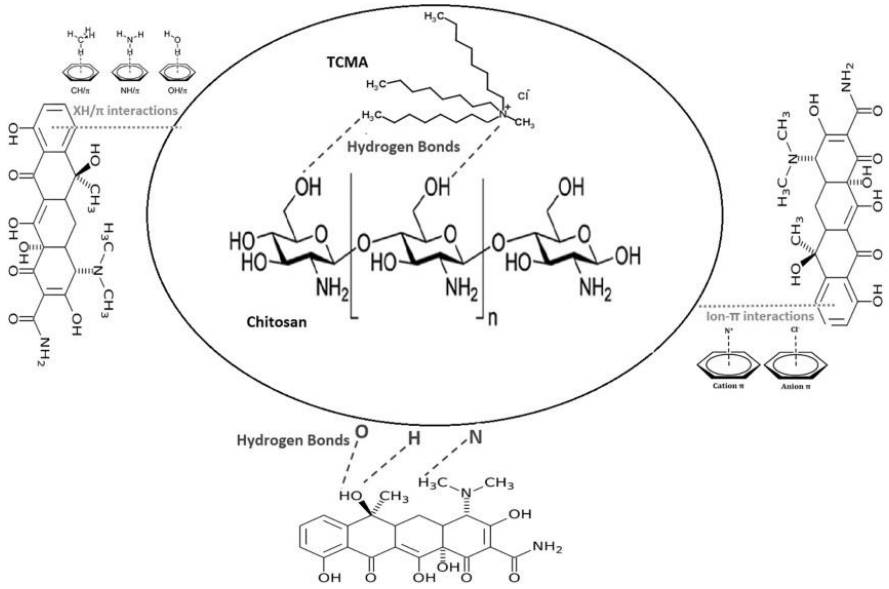

Figure 10. Schematic presenting of the structural reactions between TCMA and CS and then adsorbed molecule of TC on the surface of CS-TCMA [13].

In the study of Kyzas et al., for the removal of PRM using CsSLA adsorbent composite, the effect of humic acid on pharmaceuticals adsorption using sulfonic acid grafted chitosan was investigated. It was concluded that the interaction between CsSLA and PRM is mainly attributed to the interactions between the NH_3^+ (amino groups) of PRM and SO_3^- (sulfonic groups) of CsSLA. In addition, the presence of humic acid in the synthesized aqueous solution influences and weakens the process of adsorption (interaction between amino and sulfonic groups) due to the presence of COO^- (carboxylic groups) from humic acid. Finally, with the increase in humic acid concentration, the carboxylic groups concentration also increased, resulting in the weakening of the optimal electrostatic bond between amino and sulfonic groups [16].

In the study of Areti Tzereme et al., the adsorption of DCF from aqueous solution, using cross-linking of chitosan with trans-aconitic acid (CsTACON) etc., was investigated. FTIR spectroscopy was used to determine any possible interactions between the synthesized cross-linked adsorbents and DCF molecules. Figure 11 depicts the FTIR spectra and the characteristic functional groups of DCF at 3388, 1604, 1579, 1283, 1043, and 746 cm^{-1} peaks, which are attributed to NH stretching, C=C stretching, COO– stretching, C–Cl and C–N stretching, and C–Cl bending, respectively. After DCF sorption onto CsTACON etc., (Figure 11) the characteristic peaks of DCF and this of derivatives at 1579 cm^{-1} (strongest) were revealed.

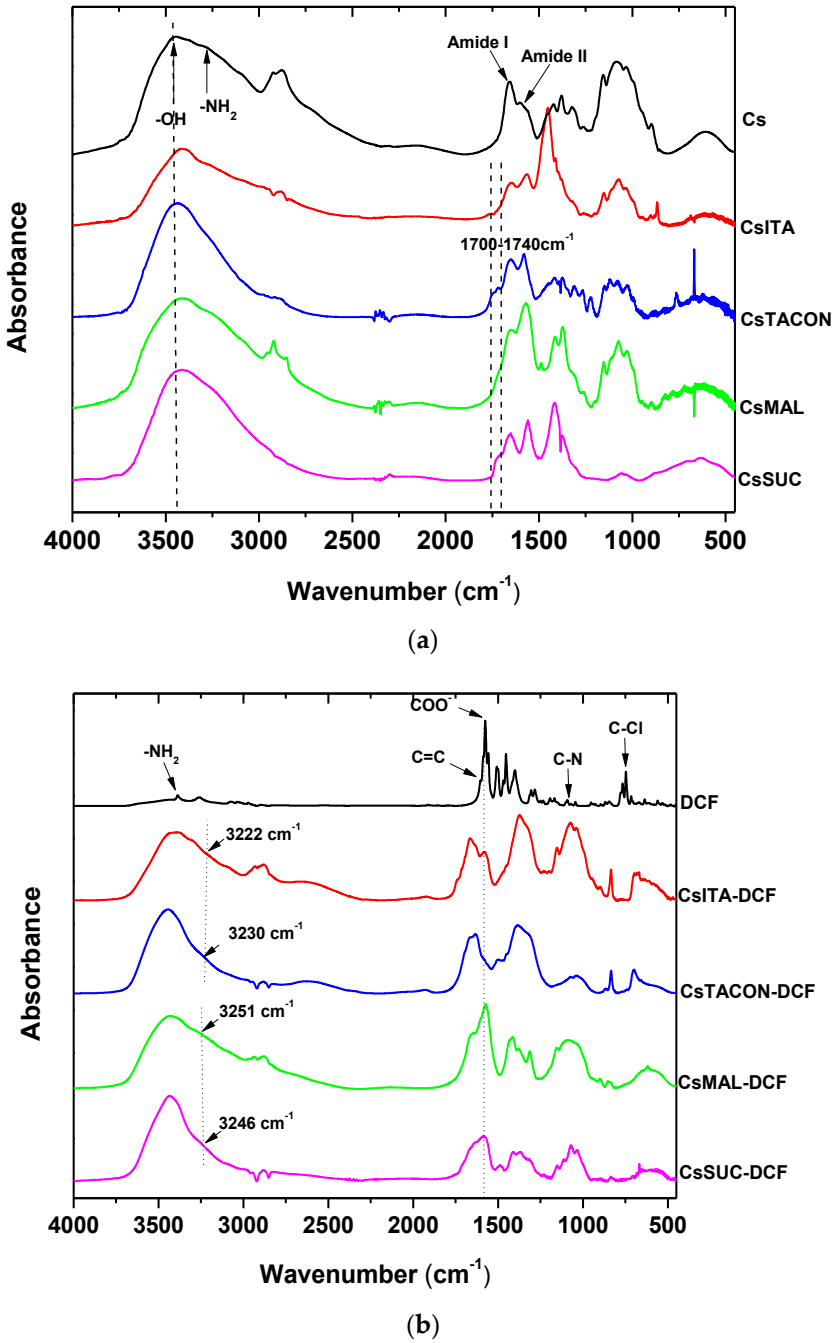

Figure 11. FTIR spectra of the synthesized chitosan derivatives: (**a**) before cross-linking in comparison with neat CS; (**b**) after cross-linking and DCF adsorption [17].

Examining the aforementioned peak (1579 cm^{-1}), it can be clearly observed that it shifted to slightly lower positions (1570–1575 cm^{-1}), for all cases of adsorbent composites, indicating that the DCF carboxylic anion interacted mainly with $–NH_2$ and possibly with the –OH groups of CS derivatives. Examining the $–NH_2$ adsorption, it can be seen that this was recorded at 3230 cm^{-1} for CsTACON-DCF. In the case of –OH adsorption, it was found that it shifted too from 3425 cm^{-1} to 3422 cm^{-1} (smaller extend than $–NH_2$ groups). Additionally, some intermolecular interactions can take place between the carboxyl groups of derivatives and those of DCF. In addition, the absorbance of $–COO^-$ was shifted from 1579 cm^{-1} to 1570–1575 cm^{-1}. However, the supposed interactions between the carboxyl groups of derivatives and secondary amino groups of DCF (>NH) have not be confirmed

from the obtained spectra after FTIR analysis, a fact which is attributed to the low-intensity absorption of >NH groups [17].

The adsorption mechanism of TC molecules onto CDF@MF adsorbent composite is based on numerous factors, such as the nature of TC, properties of CDF@MF, and the possible interactions between TC and CDF@MF. Figure 12 presents the suggested mechanism of adsorption for the adsorption of TC on the surface of CDF@MF. In addition, it was concluded that the possible interactions between TC and CDF@MF are hydrogen bonding interactions, π–π stacking interactions, and van der Waals forces [19].

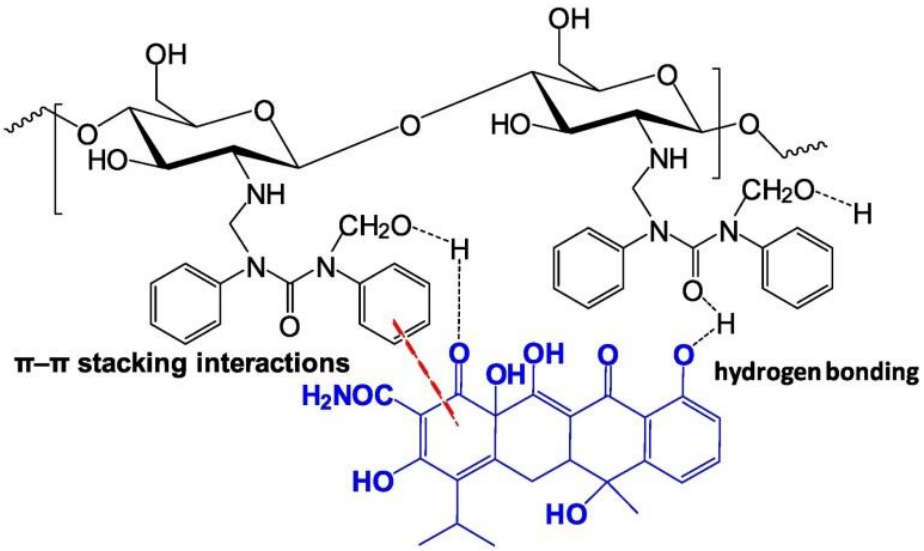

Figure 12. Mechanism of adsorption for TC onto CDF@MF [19].

The study of Shaopeng Zhang et al. investigated the adsorption of DCF and TC from aqueous solution, using CD-MCP adsorbent composite. Compared to the FTIR spectrum derived from CD-MCP adsorbent composite, a shift of the quaternary ammonium groups peak from 1377 to 1381 cm^{-1} can be observed after the adsorption of DCF and TC, indicating an electrostatic attraction between the $–N^{+}(CH_3)_3$ and anions of model pollutants [20].

Another study from Xia Zhou et al. investigated the removal of DCF, Tylosin (TYL), and Norfloxacin (NOR) from an aqueous solution, using modified CS-MCP with polycations (poly(p-vinylbenzyl trimethylammonium chloride)) branches (for DCF removal) and modified CS-MCP with polyanions (poly(sodium p-styrenesulfonate)) branches (for TYL and NOR removal). Figure 13 presents the optimization of the most stable conformations of contaminants and repeated unit complexes according to/based on the optimized structure of each single molecule. In addition, with the presence of ionic groups on branches, the preference of the ionic ends of model pollutants molecules is to get close to ionic groups with opposite charge on branches, which is attributed to electrostatic attraction. However, other fragments of model pollutant molecules can also be captured with the groups of phenyl via π-electron containing interactions (cation-π interaction for TYL, π-π interaction for DCF and NOR), which are the main reason for the enhanced pH resistance of the synthesized aromatic-ring functionalized adsorbent composites. Moreover, it must be mentioned that the π-π interaction have a much shorter bond length than cation-π interaction, indicating that the cation-π interaction is weaker [21].

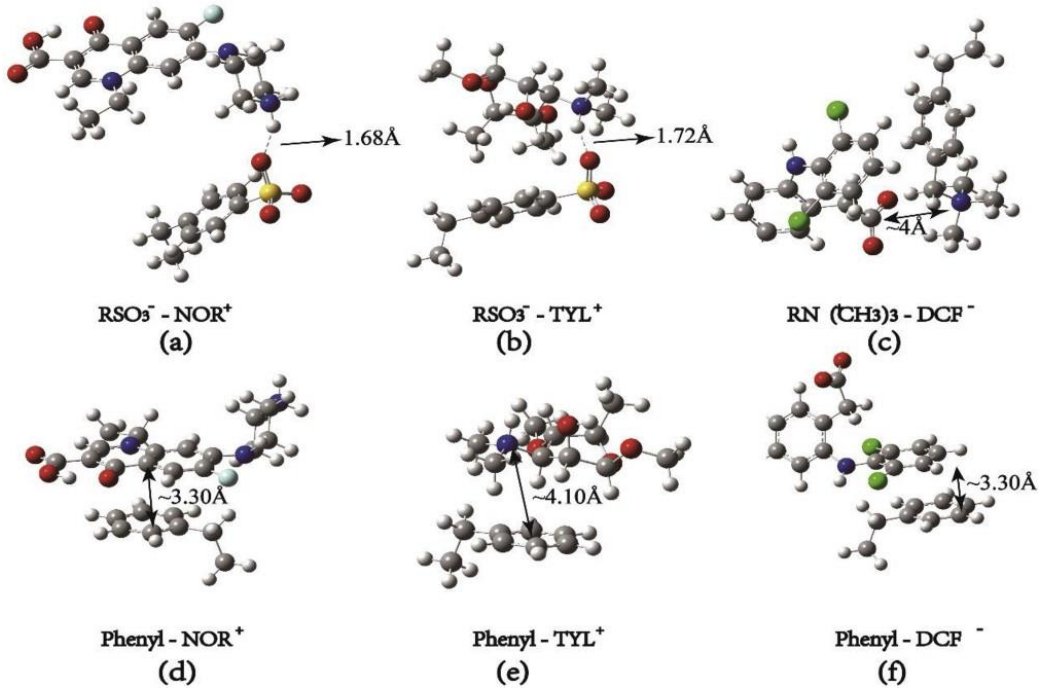

Figure 13. Optimized conformation of (**a**)RSO_3^--NOR^+, (**b**) RSO_3^--TYL^+, (**c**) RSO_3^--DCF^-, (**d**) phenyl-NOR^+, (**e**) phenyl-TYL^+, and (**f**) phenyl-DCF^- derived from DFT calculations [21].

Moreover, another study by Krithika Delhiraja et al. investigated the removal of pharmaceutical and personal care products using GO-AC-SC adsorbent composite. For further understanding of the adsorption mechanism of GO-AC-CS, the profiles of adsorption for individual components (e.g., GO, AC, and CS). More specifically, the interaction of GO with personal care products was mainly attributed to the formation of hydrogen bonds. In addition, in the case of activated carbon (AC), π-π bonds between the graphene-like flat and rings of molecules were more robust. The larger number of active centers of personal care products was found to be the main reason for the formation of π-π bonds.

However, in the case of CS, the acetaminophen and carbamazepine (pharmaceuticals) form robust bonds with the biopolymer in contrast to bisphenol A, caffeine, and triclosan (personal care products). The enhanced selectivity of CS toward acetaminophen and carbamazepine is attributed to the favorable interaction of active sites of the aforementioned pharmaceuticals and those of CS, while very few CS centers were found to be available for the formation of noncovalent bonds. However, the interaction between CS and pollutants became weaker, while the further loading of model pollutant molecules on the surface of CS resulted in a decrease in removal efficiency. In the case of GO-AC-CS adsorbent composite, the adsorbed molecules participate in the formation of hydrogen bonds between CS and GO, and also π-π bonds with AC and van der Waals bonds with CS. Furthermore, it was found that the effectiveness of the adsorption process depends mainly on the size of molecules than the number of active sites with hydrophilic or hydrophobic properties present in the personal care products. The small size of caffeine molecule (6.3 × 7.1 × 1.7 Å) was found to perfectly fit in the pores of GO-AC-CS adsorbent composite, resulting in the formation of maximal bonds. The multiple bonds' formation led to a larger H_{ads} value and enhanced capacity (10.2 mg/g). Thus, it was concluded that the molecule size is a crucial factor for the effective diffusion of molecules through the pores, indicating that the mechanism of adsorption was mainly controlled by the effectiveness of the diffusion process. Finally, the interaction between the functional groups of adsorbent composite and adsorbate also plays a role in the enhanced sorption capacity of personal care products [25].

In addition, another study by Krithika Delhiraja et al. investigated the removal of acetaminophen from synthetic wastewater using chitosan-coated MWCNTs. The adsorp-

tion mechanism of MWCNT is mainly attributed to π-π interaction mechanism due to the attractive interactions between the two π-electron orbitals and the electronic density in the aromatic ring of adsorbate and the basal plane of adsorbent via electron donor-acceptor mechanisms [29], while in the study of Xiangze Jia et al., for the removal of sulfanilamide from synthetic aqueous solution using PS-chitosan-UiO-66-COOH composite adsorbent, the adsorption mechanism was ascribed to Zr–O bond [24].

The study of Kyzas et al. investigated the uptake of dorzolamide from synthetic wastewater, using GO/CSA adsorbent composite (Figure 16).

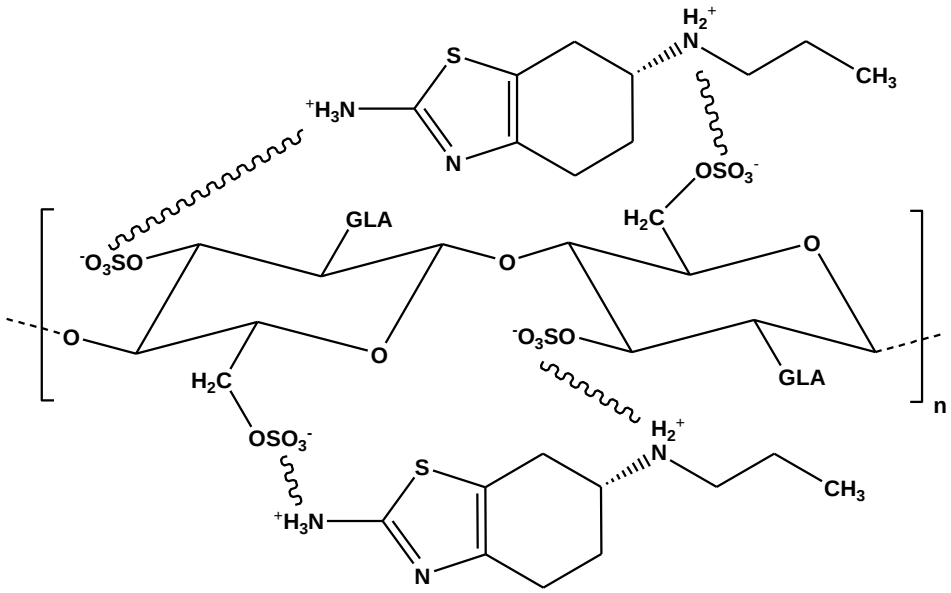

Figure 14. Interactions between CsSLF and PRM molecule [32].

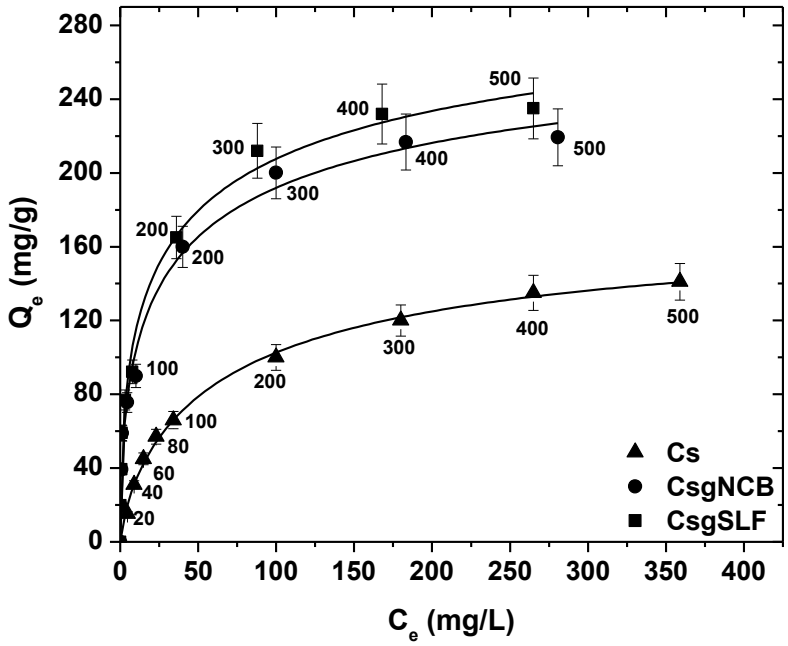

Figure 15. Effect of initial PRM concentration on adsorption onto Cs, CsNCB, and CsSLF at 25 °C [32].

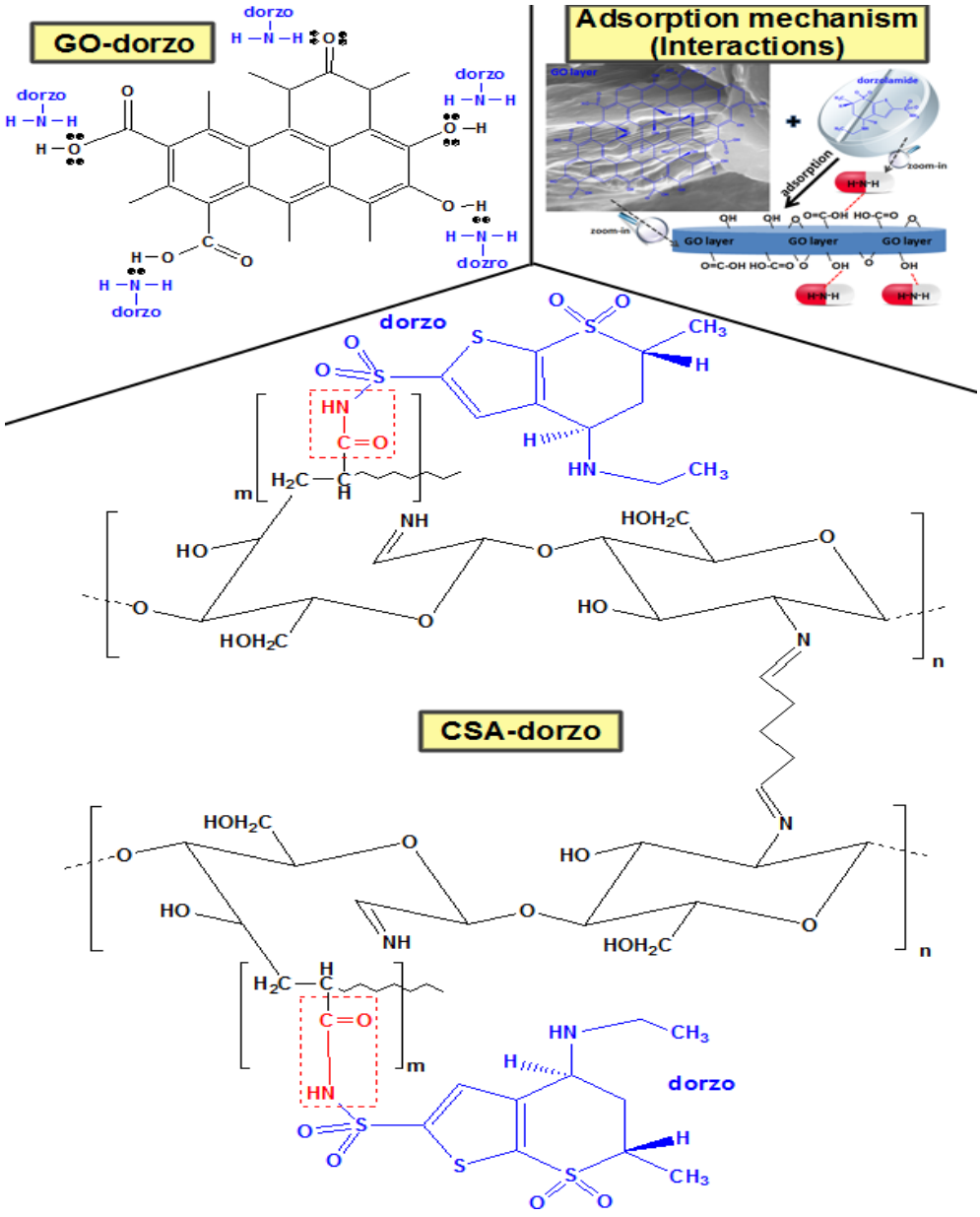

Figure 16. Adsorption mechanism and proposed interactions between dorzolamide and GO [31].

In addition, it was concluded that the mechanism for the adsorption of dorzolamide is the Lewis acid–base interaction, where the oxygen groups that contained in GO serve as Lewis acids and the dorzo $–NH_2$ is the Lewis base. In addition, the nitrogen atoms have lone pairs of electrons, resulting in the production of dipolar moments for dorzolamide. Negative charges are close to the atoms of nitrogen and the presence of GO; its surface polar oxygen groups with a lone pair of electrons may be the possible mechanism for surface-specific interactions between the dorzolamide molecules and GO oxygen surface groups (Figure 16) [31].

4. Conclusions

The use of chitosan for the synthesis of adsorbent composites, due to its increased adsorption abilities, is at its peak nowadays and many researchers worldwide focus on their synthesis. The high adsorption capacities of chitosan derivatives are attributed to the (i) grafting process, by which a wide variety of functional groups can be applied to the chemical structure of chitosan (modifiable positions), and (ii) cross-linking reactions in

order to link unit chains (each with other) with macromolecular structures. The aforementioned experimental procedures lead to the formation of chitosan composites with superior resistance in extreme media conditions and enhanced adsorption capacity. This review paper demonstrates that, in the case of pharmaceutical compounds' removal from aqueous solution, the adsorption capacity of chitosan adsorbent composite for diclofenac uptake using EPCS@PEI adsorbent composite is very high (253.32 mg/g), while in the case of tetracycline removal using GC/MGO-SO_3O adsorbent composite, the adsorption capacity was found to be even higher (473.28 mg/g). In general, the efficiency of the adsorption process depends on the pharmaceutical molecules-molecular weight, degree of dilution in synthetic aqueous solution, functional groups (adsorbent-adsorbate), temperature of aqueous solution, pH effect, etc. However, the above results of adsorption isotherms are approximately at 25 °C for all cases. Another interesting finding is that for tetracycline uptake from synthetic aqueous solutions, the best mathematic fitting of experimental data, for all cases of chitosan adsorbent composites, was achieved with the Langmuir model at pH 7–10. Finally, it can be concluded that the chitosan-based materials are very promising for the removal of a wide variety of pharmaceutical compounds (tetracycline, pramipexole, dorzolamide, diclofenac, furosemide, etc.) and personal care products (Ketoprofen, Ibuprofen, Benzoin acid, etc.) from aqueous solutions, and in the next few years are expected to be further used for various adsorption applications.

Author Contributions: Methodology, E.V.L., M.L., G.M., I.K., D.N.B., and G.Z.K.; writing—original draft preparation, E.V.L., M.L., G.M., I.K., D.A.L., D.N.B., and G.Z.K.; writing—review and editing, E.V.L., M.L., G.M., I.K., D.N.B., and G.Z.K.; supervision, D.A.L., D.N.B., and G.Z.K. All authors have read and agreed to the published version of the manuscript.

Funding: This research was funded by the Greek Ministry of Development and Investments (General Secretariat for Research and Technology) through the research project "Research-Create-Innovate", with the topic "Development of an integration methodology for the treatment of micropollutants in wastewaters and leachates coupling adsorption, advanced oxidation processes and membrane technology" (Grant no: T2EΔK-04066).

Institutional Review Board Statement: Not applicable.

Informed Consent Statement: Not applicable.

Data Availability Statement: The data presented in this study are available on request from the corresponding author.

Conflicts of Interest: The authors declare no conflict of interest.

References

1. De Andrade, J.R.; Oliveira, M.F.; Da Silva, M.G.C.; Vieira, M.G.A. Adsorption of Pharmaceuticals from Water and Wastewater Using Nonconventional Low-Cost Materials: A Review. *Ind. Eng. Chem. Res.* **2018**, *57*, 3103–3127. [CrossRef]
2. Tanhaei, B.; Ayati, A.; Iakovleva, E.; Sillanpää, M. Efficient carbon interlayed magnetic chitosan adsorbent for anionic dye removal: Synthesis, characterization and adsorption study. *Int. J. Biol. Macromol.* **2020**, *164*, 3621–3631. [CrossRef]
3. Samadi, F.Y.; Mohammadi, Z.; Yousefi, M.; Majdejabbari, S. Synthesis of raloxifene-chitosan conjugate: A novel chitosan derivative as a potential targeting vehicle. *Int. J. Biol. Macromol.* **2016**, *82*, 599–606. [CrossRef] [PubMed]
4. Fu, J.; Kyzas, G.Z.; Cai, Z.; Deliyanni, E.A.; Liu, W.; Zhao, D. Photocatalytic degradation of phenanthrene by graphite oxide-TiO_2-$Sr(OH)_2$/$SrCO_3$ nanocomposite under solar irradiation: Effects of water quality parameters and predictive modeling. *Chem. Eng. J.* **2018**, *335*, 290–300. [CrossRef]
5. Kyzas, G.Z.; Nanaki, S.G.; Koltsakidou, A.; Papageorgiou, M.; Kechagia, M.; Bikiaris, D.N.; Lambropoulou, D.A. Effectively designed molecularly imprinted polymers for selective isolation of the antidiabetic drug metformin and its transformation product guanylurea from aqueous media. *Anal. Chim. Acta* **2015**, *866*, 27–40. [CrossRef] [PubMed]
6. Kyzas, G.Z.; Bikiaris, D.N.; Mitropoulos, A.C. Chitosan adsorbents for dye removal: A review. *Polym. Int.* **2017**, *66*, 1800–1811. [CrossRef]
7. Anastopoulos, I.; Hosseini-Bandegharaei, A.; Fu, J.; Mitropoulos, A.C.; Kyzas, G.Z. Use of nanoparticles for dye adsorption: Review. *J. Dispers. Sci. Technol.* **2018**, *39*, 836–847. [CrossRef]
8. Kyzas, G.Z.; Lazaridis, N.K.; Kostoglou, M. On the simultaneous adsorption of a reactive dye and hexavalent chromium from aqueous solutions onto grafted chitosan. *J. Colloid Interface Sci.* **2013**, *407*, 432–441. [CrossRef]
9. Anastopoulos, I.; Kyzas, G.Z. Composts as biosorbents for decontamination of various pollutants: A review. *Waterairand Soil Pollut.* **2015**, *226*. [CrossRef]

10. Terzopoulou, Z.; Papageorgiou, M.; Kyzas, G.Z.; Bikiaris, D.N.; Lambropoulou, D.A. Preparation of molecularly imprinted solid-phase microextraction fiber for the selective removal and extraction of the antiviral drug abacavir in environmental and biological matrices. *Anal. Chim. Acta* **2016**, *913*, 63–75. [CrossRef]
11. Karimi-Maleh, H.; Ayati, A.; Davoodi, R.; Tanhaei, B.; Karimi, F.; Malekmohammadi, S.; Orooji, Y.; Fu, L.; Sillanpää, M. Recent advances in using of chitosan-based adsorbents for removal of pharmaceutical contaminants: A review. *J. Clean. Prod.* **2021**, *291*. [CrossRef]
12. Lu, Y.; Wang, Z.; Ouyang, X.-k.; Ji, C.; Liu, Y.; Huang, F.; Yang, L.-Y. Fabrication of cross-linked chitosan beads grafted by polyethylenimine for efficient adsorption of diclofenac sodium from water. *Int. J. Biol. Macromol.* **2020**, *145*, 1180–1188. [CrossRef] [PubMed]
13. Ranjbari, S.; Tanhaei, B.; Ayati, A.; Khadempir, S.; Sillanpää, M. Efficient tetracycline adsorptive removal using tricaprylmethylammonium chloride conjugated chitosan hydrogel beads: Mechanism, kinetic, isotherms and thermodynamic study. *Int. J. Biol. Macromol.* **2020**, *155*, 421–429. [CrossRef] [PubMed]
14. Riegger, B.R.; Bäurer, B.; Mirzayeva, A.; Tovar, G.E.M.; Bach, M. A systematic approach of chitosan nanoparticle preparation via emulsion crosslinking as potential adsorbent in wastewater treatment. *Carbohydr. Polym.* **2018**, *180*, 46–54. [CrossRef] [PubMed]
15. Rizzi, V.; Gubitosa, J.; Fini, P.; Romita, R.; Nuzzo, S.; Gabaldón, J.A.; Gorbe, M.I.F.; Gómez-Morte, T.; Cosma, P. Chitosan film as recyclable adsorbent membrane to remove/recover hazardous pharmaceutical pollutants from water: The case of the emerging pollutant Furosemide. *J. Environ. Sci. Health Part A Toxic/Hazard. Subst. Environ. Eng.* **2020**, *56*, 145–156. [CrossRef]
16. Kyzas, G.Z.; Bikiaris, D.N.; Lambropoulou, D.A. Effect of humic acid on pharmaceuticals adsorption using sulfonic acid grafted chitosan. *J. Mol. Liq.* **2017**, *230*, 1–5. [CrossRef]
17. Tzereme, A.; Christodoulou, E.; Kyzas, G.Z.; Kostoglou, M.; Bikiaris, D.N.; Lambropoulou, D.A. Chitosan Grafted Adsorbents for Diclofenac Pharmaceutical Compound Removal from Single-Component Aqueous Solutions and Mixtures. *Polymers* **2019**, *11*, 497. [CrossRef]
18. Malesic-Eleftheriadou, N.; Evgenidou, E.; Lazaridou, M.; Bikiaris, D.N.; Yang, X.; Kyzas, G.Z.; Lambropoulou, D.A. Simultaneous removal of anti-inflammatory pharmaceutical compounds from an aqueous mixture with adsorption onto chitosan zwitterionic derivative. *Colloids Surf. A Physicochem. Eng. Asp.* **2021**, 126498. [CrossRef]
19. Ahamad, T.; Ruksana; Chaudhary, A.A.; Naushad, M.; Alshehri, S.M. Fabrication of $MnFe_2O_4$ nanoparticles embedded chitosan-diphenylureaformaldehyde resin for the removal of tetracycline from aqueous solution. *Int. J. Biol. Macromol.* **2019**, *134*, 180–188. [CrossRef]
20. Zhang, S.; Dong, Y.; Yang, Z.; Yang, W.; Wu, J.; Dong, C. Adsorption of pharmaceuticals on chitosan-based magnetic composite particles with core-brush topology. *Chem. Eng. J.* **2016**, *304*, 325–334. [CrossRef]
21. Zhou, X.; Dong, C.; Yang, Z.; Tian, Z.; Lu, L.; Yang, W.; Wang, Y.; Zhang, L.; Li, A.; Chen, J. Enhanced adsorption of pharmaceuticals onto core-brush shaped aromatic rings-functionalized chitosan magnetic composite particles: Effects of structural characteristics of both pharmaceuticals and brushes. *J. Clean. Prod.* **2018**, *172*, 1025–1034. [CrossRef]
22. Liu, Y.; Liu, R.; Li, M.; Yu, F.; He, C. Removal of pharmaceuticals by novel magnetic genipin-crosslinked chitosan/graphene oxide-SO_3H composite. *Carbohydr. Polym.* **2019**, *220*, 141–148. [CrossRef]
23. Zhuo, N.; Lan, Y.; Yang, W.; Yang, Z.; Li, X.; Zhou, X.; Liu, Y.; Shen, J.; Zhang, X. Adsorption of three selected pharmaceuticals and personal care products (PPCPs) onto MIL-101(Cr)/natural polymer composite beads. *Sep. Purif. Technol.* **2017**, *177*, 272–280. [CrossRef]
24. Jia, X.; Zhang, B.; Chen, C.; Fu, X.; Huang, Q. Immobilization of chitosan grafted carboxylic Zr-MOF to porous starch for sulfanilamide adsorption. *Carbohydr. Polym.* **2021**, *253*, 117305. [CrossRef] [PubMed]
25. Delhiraja, K.; Vellingiri, K.; Boukhvalov, D.W.; Philip, L. Development of Highly Water Stable Graphene Oxide-Based Composites for the Removal of Pharmaceuticals and Personal Care Products. *Ind. Eng. Chem. Res.* **2019**, *58*, 2899–2913. [CrossRef]
26. Zhao, F.; Repo, E.; Yin, D.; Chen, L.; Kalliola, S.; Tang, J.; Iakovleva, E.; Tam, K.; Sillanpää, M. One-pot synthesis of trifunctional chitosan-EDTA-β-cyclodextrin polymer for simultaneous removal of metals and organic micropollutants. *Sci. Rep.* **2017**, *7*. [CrossRef] [PubMed]
27. Lessa, E.F.; Nunes, M.L.; Fajardo, A.R. Chitosan/waste coffee-grounds composite: An efficient and eco-friendly adsorbent for removal of pharmaceutical contaminants from water. *Carbohydr. Polym.* **2018**, *189*, 257–266. [CrossRef]
28. Feng, Z.; Danjo, T.; Odelius, K.; Hakkarainen, M.; Iwata, T.; Albertsson, A.C. Recyclable Fully Biobased Chitosan Adsorbents Spray-Dried in One Pot to Microscopic Size and Enhanced Adsorption Capacity. *Biomacromolecules* **2019**, *20*, 1956–1964. [CrossRef]
29. Yanyan, L.; Kurniawan, T.A.; Albadarin, A.B.; Walker, G. Enhanced removal of acetaminophen from synthetic wastewater using multi-walled carbon nanotubes (MWCNTs) chemically modified with NaOH, HNO_3/H_2SO_4, ozone, and/or chitosan. *J. Mol. Liq.* **2018**, *251*, 369–377. [CrossRef]
30. Kyzas, G.Z.; Matis, K.A. Nanoadsorbents for pollutants removal: A review. *J. Mol. Liq.* **2015**, *203*, 159–168. [CrossRef]
31. Kyzas, G.Z.; Bikiaris, D.N.; Seredych, M.; Bandosz, T.J.; Deliyanni, E.A. Removal of dorzolamide from biomedical wastewaters with adsorption onto graphite oxide/poly(acrylic acid) grafted chitosan nanocomposite. *Bioresour. Technol.* **2014**, *152*, 399–406. [CrossRef] [PubMed]
32. Kyzas, G.Z.; Kostoglou, M.; Lazaridis, N.K.; Lambropoulou, D.A.; Bikiaris, D.N. Environmental friendly technology for the removal of pharmaceutical contaminants from wastewaters using modified chitosan adsorbents. *Chem. Eng. J.* **2013**, *222*, 248–258. [CrossRef]